

UNIVERSITY OF MICHIGAN



**REPAIR AND STRENGTHENING OF REINFORCED CONCRETE
BEAMS USING CFRP LAMINATES**

**Volume 5: Behavior of Beams Under Cyclic Loading
at Low Temperature**

by

Antoine Naaman
Maria del Mar Lopez
Luke Pinkerton

Project Coordinator: Roger D. Till, MDOT
Project Advisor: Thomas D. Gillespie, GLCTTR

Report No. UMCEE 98 - 39
April, 1999

The University of Michigan
Department of Civil and Environmental Engineering
Ann Arbor, MI 48109-2125, USA

Technical Report Documentation Page

1. Report No. RC - 1372	2. Government Accession No.	3. Recipient's Catalog No.	
4. Title and Subtitle Repair and Strengthening of Reinforced Concrete Beams using CFRP Laminates. Volume 5: Behavior of Beams under Cyclic Loading at Low Temperature		5. Report Date April, 1999	
7. Author (s) Antoine E. Naaman Maria del Mar Lopez Luke Pinkerton		6. Performing Organization Code UMCEE 98 - 39	
9. Performing Organization Name and Address The University of Michigan, Dept. of Civil and Env. Engineering 2340 G.G. Brown Bldg. Ann Arbor, MI 48109-2125		8. Performing Org Report No. RC - 1372	
12. Sponsoring Agency Name and Address Michigan Department of Transportation Construction and Technology Division P.O. Box 30049 Lansing, MI 48909		10. Work Unit No. (TRAIS)	
		11. Contract/Grant No.	
15. Supplementary Notes		13. Type of Report & Period Covered Research Report 1997-1998	
		14. Sponsoring Agency Code	
16. Abstract			
<p>Repair and strengthening techniques using glued-on carbon fiber reinforced plastic (CFRP) plates (also called sheets, tow sheets, and thin laminates) form the basis of a new technology being increasingly used for bridges and highway superstructures.</p> <p>The study described in this report (Volumes 1 to 7) focused on the use of carbon fiber reinforced plastic (CFRP) laminates for repair and strengthening of reinforced concrete beams. Its primary objectives are: 1) to ascertain the applicability of CFRP adhesive bonded laminates for repair and strengthening of reinforced concrete beams; 2) to synthesize existing knowledge and develop procedures for implementation in the field; 3) to identify key parameters for successful design and implementation; and 4) to adapt this technique to the specific conditions encountered in the state of Michigan.</p> <p>This report consists of 7 volumes: Volume 1 – Summary Report Volume 2 – Literature Review Volume 3 – Behavior of Beams Strengthened for Bending Volume 4 – Behavior of Beams Strengthened for Shear Volume 5 – Behavior of Beams Under Cyclic Loading at Low Temperature Volume 6 – Behavior of Beams Subjected to Freeze-Thaw Cycles Volume 7 – Technical Specifications</p> <p>The part of the investigation dealing with the tests in bending and shear of strengthened beams under low temperature (-29° C) and high amplitude cyclic loading is the subject of this volume (volume 5). Results are also analyzed, compared, and discussed. Four reinforced concrete beams strengthened with CFRP sheets were designed, prepared and tested under low temperature conditions (-29°C). Two beams were tested monotonically to failure and the other two were tested under high amplitude cyclic load (fatigue load). Parameters investigated were: Low temperature and loading conditions. The four beams were tested under low temperature conditions (-29°C). Two beams were tested under a four-point load configuration, one monotonically and one in cyclic fatigue. These beams, considered to fail in bending, were strengthened with the Sika system. The remaining two beams were tested under three-point load configuration, also one monotonically and one in cyclic fatigue. These beams considered to fail in shear were retrofitted with the Tonen system. The amplitude of the cyclic fatigue load was taken as 10-80% of the failure load from the monotonic test. Conclusions are drawn and some recommendations for design are suggested.</p>			
17. Keywords bond, carbon fiber, composites materials, laminates, rehabilitation, reinforced concrete, repair, strengthening systems		18. Distribution Statement No restrictions. This document is available to the public through the Michigan Department of Transportation	
19. Security Classification (report) Unclassified	20. Security Classification (Page) Unclassified	21. No. of pages	22. price

Michigan Department of Transportation - Technical Advisory Group

Roger D. Till, *Project Coordinator*
Materials and Technology Laboratories

David Juntunen
Materials and Technology Laboratories

Jon Reincke
Materials and Technology Laboratories

Glenn Bukoski
Construction

Steve Beck
Design

Raja Jildeh
Design

Michel Tarazi
Design

Steve O'Connor
Engineering Services

Sonny Jadun
Maintenance

John Nekritz
Federal Highway Administration

Great Lakes Center for Trucks and Transit Research

Thomas D. Gillespie, *Project Advisor*
University of Michigan Transportation Research Institute

University of Michigan - CEE Research Team

Antoine Naaman, *Project Director*

Sang Yeol Park, *Research Fellow*

Maria del Mar Lopez, *Graduate Research Assistant*

Luke R. Pinkerton, *Graduate Research Assistant*

UMCEE 98 - 39
MDOT Contract No: 96-1067BAB

Project Director: Antoine E. Naaman, UM
Project Coordinator: Roger D. Till, MDOT
Project Advisor: Thomas D. Gillespie, GLCTTR

December 10, 1998

key words:

adhesives
bending
bond
carbon fiber
composite materials
concrete
durability
epoxy
fatigue
freeze thaw
FRP sheets
low temperature
repair
rehabilitation
shear
strengthening systems

Department of Civil and Environmental Engineering
University of Michigan, 2340 G.G. Brown building
Ann Arbor, MI 48109-2125
Tel: 1-734-764-8495; Fax: 1-734-764 4292

The publication of this report does not necessarily indicate approval or endorsement of the findings, opinions, conclusions, or recommendations either inferred or specifically expressed herein, by the Regents of the University of Michigan, the Michigan Department of Transportation, or the Great Lakes Center for Trucks and Transit Research.

ACKNOWLEDGMENTS

The research described in this report was supported jointly by a grant from the Michigan Department of Transportation and the Great Lakes Center of Truck and Transit Research which is affiliated with the University of Michigan Transportation Research Institute. Matching funds for student tuition and for equipment were also provided by the University of Michigan.

The research team received valuable support, counsel, and guidance from the Technical Advisory Group. The support and encouragement provided by Roger Till, project coordinator representing the Michigan Department of Transportation, is deeply appreciated.

The authors are thankful to the Sika Corporation (Bob Pisha) for the donation of the Carbodur laminate as well as the Sikadur epoxy material. The partial contribution of Tonen Corporation with the MBrace composite strengthening system, and the help of Howard Kliger are also appreciated.

The opinions expressed in this report are those of the authors and do not necessarily reflect the views of the sponsors.

TABLE OF CONTENTS

ACKNOWLEDGMENTS	iii
LIST OF FIGURES.....	vi
LIST OF TABLES	vi
PREFACE	vii
ABSTRACT	viii
EXECUTIVE SUMMARY	ix
1. INTRODUCTION.....	1
1.1. Organization of this Report.....	1
2. EXPERIMENTAL PROGRAM	2
2.1. Parameters of study	2
2.2. Material Properties	2
2.2.1. Concrete.....	2
2.2.2. Reinforcing bars.....	4
2.2.3. Strengthening Systems	4
2.3. Design and Fabrication of Specimens.....	5
2.3.1. Flexural Beams	5
2.3.2. Shear Beams.....	6
2.3.3. CFRP Application.....	6
2.4. Test Set-Up and Instrumentation	7
3. DESIGN OF TEMPERATURE CONTROL SYSTEM.....	11
3.1. Liquid Nitrogen Cooling System	11
3.1.1. Specimen Cooling Apparatus	11
3.1.2. Automatic Liquid Nitrogen Delivery System	11
3.1.3. Insulation.....	14
3.1.4. Performance.....	15
4. TEST RESULTS	15

5. ANALYSIS AND INTERPRETATION	18
5.1. Steel Reinforcement Ratio.....	18
5.2. Failure Modes.....	18
5.2.1. <i>Flexure Test</i>	18
5.2.2. <i>Shear Test</i>	19
5.3. Strengthening Level.....	27
5.4. Temperature and Fatigue Effect.....	33
6. CONCLUSIONS	36
7. REFERENCES WITH SOURCE CLASSIFICATION	36
8. APPENDIX A	39

LIST OF FIGURES

Figure 2.1 Cross Section and Load Set-Up for Shear (top) and Bending (bottom) Test	9
Figure 2.2 Strain Gage Layout for the Shear and Bending Tests.....	10
Figure 3.1 Photograph of the Hollow Shear Specimens before Concrete Pouring	12
Figure 3.2 Photograph of Coolant Tubes.....	12
Figure 3.3 Flexural Specimen Cooling System.	13
Figure 3.4 Shear Specimen Cooling System.	13
Figure 3.5 Temperature control Loop.....	14
Figure 4.1 Load versus Deflection Curve for Monotonic Bending Test.....	17
Figure 4.2 Load versus Deflection Curves for Fatigue Bending Test.....	17
Figure 4.3 Load versus Deflection Curve for Monotonic Shear Test	18
Figure 4.4 Load versus Deflection Curves for Fatigue Shear Test	18
Figure 5.1 Interfacial Failure of the Monotonic Bending Specimen	21
Figure 5.2 Detail of the Interfacial Failure of the Monotonic Bending Specimen.....	21
Figure 5.3 Load versus Strain Curves for Monotonic Flexure Test.....	22
Figure 5.4 Interfacial Failure of the Fatigue Flexure Test	23
Figure 5.5 Detail of the Interfacial Failure of the Fatigue Flexure Test	23
Figure 5.6 Interlaminar Failure at the End of the Sika Plate (Fatigue Flexure).....	23
Figure 5.7 Load versus Strain Curves for Monotonic after Cycling Flexure Test.....	24
Figure 5.8 Shear Failure and Debonding of the Tonen CRP sheet	25
Figure 5.9 Detail of the Debonded Area (Shear Monotonic).....	25
Figure 5.10 Load versus Shear Strain Curves from the Monotonic Shear Test.....	26
Figure 5.11 Brittle Failure of the Shear Cyclic Specimen	28
Figure 5.12 Detail of the Brittle Failure of the Shear Cyclic Specimen	28
Figure 5.13 Brittle Failure of a Steel Rebar (bar No. 3)	29
Figure 5.14 Brittle Failure of a Steel Rebar (bar No. 4)	29
Figure 5.15 Load versus Shear Strain Curves from the Fatigue Shear Test	30
Figure 5.16 Load versus Deflection Curves for Monotonic and Fatigue Bending Tests.....	30
Figure 5.17 Load versus Stress Curves for Monotonic Flexure Test.....	35
Figure 5.18 Load versus Stress Curves for Monotonic after Cycling Bending Test.....	35

LIST OF TABLES

Table 2.1 Test Parameters for Low Temperature and Fatigue Load Conditions	2
Table 2.2 Proportions of the Concrete Mix	3
Table 2.3 Compression Test Results	3
Table 2.4. Test parameters for bending and shear tests	7
Table 2.5 Summary of the Fatigue Tests Procedure	8
Table 3.1 Control Thermocouples and Average Temperatures.....	15
Table 4.1 Summary of the Test Results.....	16
Table 5.1 Summary of the Test Results.....	18
Table 5.2 Interfacial Shear Values for the Bending Tests	31
Table 5.3 Shear Contribution of the CFRP sheet	32

PREFACE

This project titled: "*Repair and Strengthening of Reinforced Concrete Beams using CFRP Laminates*" is aimed at providing experimental verification and recommendations for implementation of a new technology, in which thin fiber reinforced plastic laminates are glued-on the surface of concrete beams in order to strengthen them.

The primary objectives of the project were:

- To ascertain the applicability of Carbon Fiber Reinforced Plastic (CFRP) glued-on plates for repair and strengthening of concrete beams;
- To synthesize existing knowledge and develop procedures for implementation in the field;
- To adapt this technique to the specific conditions encountered in the state of Michigan.

The project consisted of 8 tasks as follows:

- A report containing a literature review and a comprehensive synthesis of the latest state of knowledge on the glued -on FRP technique (Task 1);
- Laboratory testing and verification of the selected CFRP glued-on technique according to the proposed experimental program: bending (Task 2), shear (Task 3), freeze-thaw (Task 4), temperature and high cyclic amplitude load (Task 5);
- An interim and final report summarizing the experimental results (Task 6). The interim report will cover the bending and freeze-thaw tests;
- A summary of field specifications and "how to" details for implementation in field applications;
- Guidelines for design based on the experience developed from the experimental work (Task 7);
- Field monitoring of application of the technique to one bridge selected by MDOT (Task 8a);
- Bridge testing before and after application of the glued-on plate (Task 8b to be conducted by professor A. Nowak, U of M)

This report summarizes the experimental program of beams under cycling loading at low temperature as per Task 5.

ABSTRACT

Repair and strengthening techniques using glued-on carbon fiber reinforced plastic (CFRP) plates (also called sheets, tow sheets, and thin laminates) form the basis of a new technology being increasingly used for bridges and highway superstructures.

The study described in this report is part of a larger investigation on the use of carbon fiber reinforced plastic (CFRP) sheets for repair and strengthening of reinforced and prestressed concrete beams. Its primary objectives are: 1) to ascertain the applicability of CFRP glued-on plates for repair and strengthening of concrete beams, 2) to synthesize existing knowledge, 3) to identify optimum parameters for successful implementation, 4) to develop procedures for implementation in the field, and 5) to adapt the technique to the specific conditions encountered in the state of Michigan.

The experimental program includes four main parts: 1) tests of RC beams strengthened in bending; 2) tests of RC beams strengthened in shear; 3) freeze-thaw tests of strengthened beams followed by their test in bending; and 4) tests in bending and shear of strengthened beams under low temperature (-29°C) and high amplitude cyclic loading.

The part of the investigation dealing with the tests in bending and shear of strengthened beams under low temperature (-29°C) and high amplitude cyclic loading is the subject of this report. Results are also analyzed, compared, and discussed. Four reinforced concrete beams strengthened with CFRP sheets were designed, prepared and tested under low temperature conditions (-29°C). Two beams were tested monotonically to failure and the other two were tested under high amplitude cyclic load (fatigue load). Parameters investigated were: Low temperature and loading conditions. The four beams were tested under low temperature conditions (-29°C). Two beams were tested under a four-point load configuration, one monotonically and one in cyclic fatigue. These beams, considered to fail in bending, were strengthened with the Sika system. The remaining two beams were tested under three-point load configuration, also one monotonically and one in cyclic fatigue. These beams considered to fail in shear were retrofitted with the Tonen system. The amplitude of the cyclic fatigue load was taken as 10-80% of the failure load from the monotonic test. Conclusions are drawn and some recommendations for design are suggested.

The experience gained during this project should contribute to a better understanding of the behavior of these new strengthening systems under different environmental conditions.

EXECUTIVE SUMMARY

This report presents the summary of experimental work, laboratory testing, and analysis of results for task 5 of the current research project which deals with the tests in bending and shear of strengthened beams under low temperature (-29° C) and high amplitude cyclic loading. Results are also analyzed, compared, and discussed.

Based on the results from the experimental work, the following conclusions were drawn:

1. Prior tests (Task 2) showed that the failure mode of RC beams strengthened with CFRP Sika plates and loaded in monotonic bending at normal room temperature was by delamination of the CFRP plate. The limited tests carried out in this task with low temperature (-29 °C) and cyclic fatigue loading, suggest that the failure mode remains the same, that is by delamination.
2. The strain data of the cyclic fatigue test in bending showed redistribution of strains (thus stresses) in the CFRP plate with an increasing number of cycles. A more uniform strain pattern was achieved suggesting that slow delamination of the plate occurred during cycling. Higher strains at the end of the plate confirmed the extension of delamination toward that section and subsequent delamination failure at that section.
3. Values of the interfacial shear stress from the strains recorded by the gages showed that the interfacial strength at failure was similar for both the monotonically flexure tested beam (1.62 MPa) and the fatigue flexure beam after 155,500 cycles (1.58 MPa).
4. Failure in the shear beam subjected to monotonic loading at -29 °C occurred by shear delamination of the CFRP Tonen sheet followed by shear failure of the concrete. The shear delamination was due to the propagation of a diagonal shear crack within the concrete that extended from the load point to the supports.
5. Failure in the shear beam that was subjected to cyclic fatigue loading at -29 °C was initiated by failure of one of the reinforcing bars in the first layer of steel, and shortly followed by failure of two additional bars. Subsequent analysis suggested that failure of the rebars was by brittle fracture.
6. Increase in the shear strain obtained with cyclic shear loading from the rosette gage placed at midspan along the vertical axis of the beam suggest that some delamination and cracking were occurring at that section. It is likely that a shear failure would have occurred in a manner similar to the monotonically tested beam, should failure of the reinforcing bar not have occurred.

1. INTRODUCTION

This study is part of a research project at the University of Michigan supported by the Michigan Department of Transportation and the Great Lakes Center for Truck and Transit Research. The project title is "Repair and Strengthening of Reinforced and Prestressed Concrete Beams Using Carbon Fiber Reinforced Plastic (CFRP) Glued-on Plates". The study is aimed at providing experimental verification and recommendations for implementation of a new technology, in which thin fiber reinforced plastic laminates are glued-on the surface of concrete beams in order to strengthen them.

The primary objectives of this project are to ascertain the applicability of CFRP glued-on plates for repair and strengthening of concrete beams, to synthesize existing knowledge and develop procedures for implementation in the field, and to adapt this technique to the specific conditions encountered in the State of Michigan. The project consists of 8 tasks. Task 5 deals with the flexural and shear testing of reinforced concrete beams with glued-on CFRP plates subjected to low temperature and high amplitude load. It was of the interest of this research project to test the effectiveness of this strengthening system in cold temperatures as well as fatigue loads, both situations that could be encountered during the service life of a structure strengthened with externally glued-on CFRP plates. This is the subject of this report.

1.1. Organization of this Report

This report presents the summary of experimental work, laboratory testing, and analysis of the results for Task 5 of the current research project: Flexural and shear testing of reinforced concrete beams with glued-on CFRP plates subjected to low temperature and high amplitude cyclic load.

Chapter 2 presents the experimental program. The main experimental parameters, the material properties, fabrication of specimens, and test set-up and instrumentation are described.

Chapter 3 summarizes the procedure followed to test the specimens under low temperature conditions. Design of a controller system is explained.

Chapter 4 presents the results from the bending and shear tests of specimens subjected to low temperature and high amplitude load.

Chapter 5 presents the interpretation and analysis of the experimental results.

Chapter 6 presents the conclusions based on this experimental study.

Chapter 7 provides a list of references.

Chapter 8 includes Appendix A: Design example

2. EXPERIMENTAL PROGRAM

2.1. Parameters of study

Four reinforced concrete beams strengthened with CFRP sheets were designed, prepared and tested under low temperature conditions (-29°C). Two beams were tested monotonically to failure and the other two were tested under high amplitude cyclic load (fatigue load).

Parameters investigated were:

- 1) Low Temperature. The four beams were tested under low temperature conditions (-29°C).
- 2) Loading conditions.

Two beams were tested under a four-point load configuration, one monotonically and one in cyclic fatigue. These beams, considered to fail in bending, were strengthened with the Sika system. The remaining two beams were tested under three-point load configuration, also one monotonically and one in cyclic fatigue. These beams, considered to fail in shear, were retrofitted with the Tonen system.

The amplitude of the cyclic fatigue load was taken as 10-80% of the failure load from the monotonic test.

Table 2.1. presents the summary of the parameters tested.

Table 2.1 Test Parameters for Low Temperature and Fatigue Load Conditions

Beam Description	Temperature	Type of Loading
Bending Testing	-29°C	Monotonic to failure
Bending Testing	-29°C	High amplitude cycling (10% to 80% of ultimate bending strength)
Shear Testing	-29°C	Monotonic to failure
Shear Testing	-29°C	High amplitude cycling (10% to 80% of ultimate shear strength)

2.2. Material Properties

2.2.1. Concrete

The beams were fabricated in the structural lab of the Department of Civil and Environmental Engineering at the University of Michigan. Concrete was ordered from a ready mix concrete company. Specifications for the mix were provided to the ready mix company: Portland cement type I, sand type 2NS were used as well as a coarse aggregate (source: Stoneco Stone

Co.) with size and gradation corresponding to a 26A and a dilation number (0.0023) that meet MDOT requirements regarding freeze-thaw dilation (MTM 113-97). Two additives were provided: an air entraining agent, in order to obtain a minimum air content of $6.5\% \pm 1.5\%$ according to MDOT requirements, and a superplasticizer for better workability of the mix during placement. The specified compressive strength was 34.5 MPa.

The mix proportions of the concrete as provided by the supplier are presented in Table 2.2.

Table 2.2 Proportions of the Concrete Mix

Materials	Proportions (Kg/m ³)
Cement Type I	390
Sand (2NS)	759
Limestone (26A)	1020
Water	148
Superplasticizer (Daracem 55)	1528 ml/m ³
Air Entraining Agent (Darex II)	383 ml/m ³

The properties of the fresh concrete were as follows:

- Air content. The volume of air contained in the concrete mix was measured using a roll-a-meter. The average value obtained was 5%, which falls within the admissible range.
- Slump > 254 mm (note: this high value of slump may be caused by the addition of excessive superplasticizer by the ready mix company. As indicated below, the compressive strength of the concrete was below the target value of 34.48 MPa)

The actual compressive strength was obtained from cylinders (102 mm diameter, 203 mm height) tested at the time of testing of each beam specimen. Average values (of two cylinders tested) are presented in Table 2.3.

Table 2.3 Compression Test Results

Date	Description	Age at testing	Compressive Strength (MPa)
May 20, 1998	Pouring of Concrete	-	-
May 28, 1998	Application CFRP	7 days	19.65
June 4, 1998	Monotonic shear	15 days	23.24
June 5-8, 1998	Fatigue shear	15 days	23.24
June 11, 1998	Monotonic flexure	21 days	24.13
July 23-August 3, 1998	Fatigue flexure	60 days	30.49

2.2.2. Reinforcing bars

The steel reinforcing bars were Grade 420 with minimum yield strength of 420 MPa and a tensile modulus of 200 GPa. Two diameter were used, 10 mm (No. 10) and 13 mm (No.13).

2.2.3. Strengthening Systems

2.2.3.1. Tonen System

The strengthening system was supplied by Master Builders. Commercial name: MBrace Composite Strengthening System. It has five components:

- MBrace Primer
- MBrace Putty filler (not used)
- MBrace Saturant Resin
- MBrace Fiber Reinforcement (MBrace CF130 Carbon fiber system)
- MBrace Topcoat (not used)

MBrace Putty filler was not used since it is intended to be used to patch cracks and the concrete used did not required this surface preparation. MBrace Topcoat is an optional finishing layer for painting appearance and UV protection. Since the testing of the beams was to be performed indoors, this finishing was not used on this experimental program.

Typical Properties of MBrace CF 130 (provided by the supplier):

Fiber Reinforcement: Carbon Fiber, High Tensile

Fiber Density: 1.82 g/cm³

Fiber Modulus: 2.35 x10⁶ kg-force/cm²

Fiber Areal Weight Density: 300g/m²

Sheet Width: 50 cm

Tensile Strength: 590 kg-f/cm-sheet width

35,500 kg-f/cm²

Tensile Modulus: 38,800 kg-f/cm-sheet width

2.35 x10⁵ kg-f/cm²

Design Thickness: 0.165 mm/ply

Tensile Elongation at ultimate: 1.5%

Typical Properties of MBrace Saturant (provided by the supplier):

Volatile Organic Compounds: 20 g/liter

Flash Point: 72°C

Mixed Viscosity @ 20°C: 1,600 cps

Color: Blue

Weight/Gallon: 1.04±0.024 kg/L

Shelf Life @ 20°C: 18 months

Flexural Strength: 43 MPa

Tensile Strength: 78 MPa

Compressive Strength: 88 MPa

Work Time @ 20°C: 30 minutes

Typical Properties of MBrace Primer (provided by the supplier):

Generic type: Amine-cured liquid epoxy

Solids content: 100%

Color: clear Amber

Weight/Gallon: Part A 1139g/L

Part B 996 g/L

Tensile Strength: 13 to 15.8 MPa

Tensile Modulus (Tangent): 689 to 826.8 MPa

Tensile elongation: 20-30%

Tensile bond strength (steel): 17 MPa

Work Time @ 20°C: 45 hours

2.2.3.2. Sika System

The Sika Company provided the strengthening system. Components of this system are:

- Sika Carbodur CFRP (Carbon fiber laminate strips).
- Sikadur 30 (epoxy adhesive).

Typical Properties of Sika CFRP Strips (provided by the supplier):

Tensile Strength: 2,400 MPa

Modulus of Elasticity: 150×10^3 MPa

Density: 1.6 g/cm³

Thickness: 1.2 mm

Sheet width: 50 or 80 mm

Elongation at ultimate: 1.4%

Typical Properties of Sikadur 30 (provided by the supplier):

Application Temperature: 18-30°C

Pot Life @23°C: 70 min

Compressive Strength (14 day) > 58.6 MPa

Shear Strength: 24.8 MPa

Tensile Strength @7 day: 24.8 MPa

Elongation at break: 1%

2.3. Design and Fabrication of Specimens

2.3.1. Flexural Beams

The issue of cooling the specimens during testing was addressed before design of beams. A square hollow covered section was considered to be the most efficient for achieving a uniform low temperature. A cross section of 203 mm x 203 mm with a centered hollow core of 76 mm diameter was chosen. The cooling process was provided by injection of liquid nitrogen in the

hollow section. Specific details of the design of the cooling system will be provided in the next section.

The design of the specimens for flexural tests was based on the results from the previous bending tests (Task 2). The span to depth ratio (l/d) was intended to be similar to the one used for the previous tests, $l/d=12.58$. The beams had a length of 1981 mm. Longitudinal steel was designed such as for a compressive strength of 34.5 MPa, the reinforcement ratio will be $2/3$ of ρ_{max} . At the time of testing of each specimen, it was found that the compressive strength of the concrete was different than the specified value. Corrected steel reinforcement ratios as a percent of ρ_{max} are presented in Table 2.4. It was assumed that the aluminum tube used to cast the hollow section did not provide any contribution to the flexural strength of the specimen and did not affect its strength.

The test beams had four longitudinal reinforcing bars, placed in two rows. The lower row had two No. 13 bars centered at 38 mm from the bottom fiber. The upper row had one bar No. 13 and one bar No. 10 with a center to center distance of 38 mm from the lower row. Two additional No. 10 bars were provided in a top layer located 38 mm from the top fiber of concrete. To ensure flexural failure with the addition of the CFRP laminate, sufficient stirrups were provided (see Appendix A). The cross sections of these beams as well as load set-up are presented in Figure 2.1.

Wood molds were utilized for the fabrication of the specimens. Thermocouples were placed at different locations in order to record the temperature during the testing. A more detailed description of the location of thermocouples is given in the next section.

2.3.2. Shear Beams

Shear beams had the same cross section as the flexure beams. Longitudinal steel was also placed in the same way as for the flexure beams (see previous section). No stirrups were provided in order to measure the contribution of the CFRP system to shear resistance. It was assumed that the aluminum tube used to cast the hollow section did not affect the shear strength of the specimen.

The shear span to depth ratio (a/d) of 2.5 was the same as that used in the previous shear tests (Task 3). The total length of the shear beams was 1016 mm. Load set-up for the shear specimens is presented in Figure 2.1.

2.3.3. CFRP Application

All surfaces of the specimens that were going to receive a CFRP sheet were ground with a disk grinder. The concrete surface was ground enough to remove laitance and show the open texture of the aggregates. After grinding the dust was removed by brushing and vacuum cleaning.

Table 2.4. Test parameters for bending and shear tests

Beam No.	Test parameter	Reinforcement ratio, ρ	A_s (used) mm^2	Effective depth (mm)	CFRP reinforcement
1	Monotonic shear	$0.89 \rho_{\max}$	3#10 1#13 $A_s = 458$	$d_s = 141$ $d_f = 203$	Shear reinf: 1 layer Tonen sheet
2	Fatigue shear	$0.89 \rho_{\max}$			
3	Monotonic flexure	$0.85 \rho_{\max}$			Flexural reinf: 1 layer Sika plate
4	Fatigue flexure	$0.70 \rho_{\max}$			

The Tonen sheets and the Sika plate were cut to proper lengths using a sharp blade and a disk cutter, respectively. The adhesive components were mixed according to the technical data sheet provided by the respective system supplier. Application of each strengthening system followed the supplier recommendations.

The reinforced concrete beams were not precracked before the application of the CFRP material.

A Sika CFRP plate of 102 mm width and 1753 mm length was placed at the bottom side of the flexural beam specimens (see Figures 2.1 and 2.2). The width and length of the CFRP plate were calculated in order to obtain the maximum strengthening. A summary of these preliminary calculations is presented in Appendix A.

For the shear beams, CFRP Tonen sheets were used as the only shear reinforcement. One layer of CFRP sheet was wrapped around the lateral sides (U-shape) of the beam along its total span length (711 mm) as shown in Figures 2.1 and 2.2. Two Tonen sheets of 432 mm width (77 mm overlap at the midspan) and 609 mm length were used on each specimen. The direction of the fibers was perpendicular to the longitudinal axis of the beams.

2.4. Test Set-Up and Instrumentation

A computer based data acquisition system (Megadack System) was used to measure load and displacement of the machine load cell and machine LVDT, as well as strains from the CFRP sheets and plates.

For the flexure tests, six strain gages were placed along the length of the CFRP plate. Two strain gages were placed at midspan (M1, M2), two strain gages were placed at about one third of the span (R2 on the right side and L2 on the left side), and two strain gages were placed at 267 mm from both ends of the CFRP plate (R1 on the right side and L1 on the left side), see Figure 2.2.

For the shear tests, six strain gages in a rosette configuration were placed on one of the lateral sides of each beam. Three rosette strain gages were placed in a vertical arrangement at 178 mm

from each end of the CFRP wrap (for the right side: TR top right, MR middle right, BR bottom right; for the left side TL top left, ML middle left, BL bottom left). Location and numbering of the strain gages for each particular test are shown in Figure 2.2.

The two beams that were tested monotonically to failure were loaded using displacement control at a loading rate of 0.13 mm/second. The Instron machine load cell used has a capacity of 450 kN.

The two beams that were tested under fatigue were loaded using load control at a frequency of 3 cycles/second. The target range of testing was 10-80% of the ultimate load from the monotonic test.

Due to safety measures of the structure lab, the fatigue tests had to be stopped at the end of each testing day. The fatigue test of the shear beam was completed in two days. The fatigue test of the bending beam was completed in three days. At the beginning of the third day it was decided to increment the loading range to 10-90%. At the end of the day, and due to the fact that no change was observed in the behavior of the beam, the range was increased to 10-100% during 10,000 cycles. Finally, the beam was tested monotonically to failure under displacement control. Table 2.5 presents a summary of the testing stages for both fatigue tests.

Table 2.5 Summary of the Fatigue Tests Procedure

Test	Cycles (accumulative)	Date	Cycle
Shear Fatigue	0-28902	June 5, 1998	10-80%
	28903-43083	June 8, 1998	10-80%
Bending Fatigue	0-30000	July 23, 1998	10-80%
	30001-85000	July 24, 1998	10-80%
	85001-145999	August 3, 1998	10-90%
	146000-15499	August 3, 1998	10-100%
	155500	August 3, 1998	Monotonic to failure

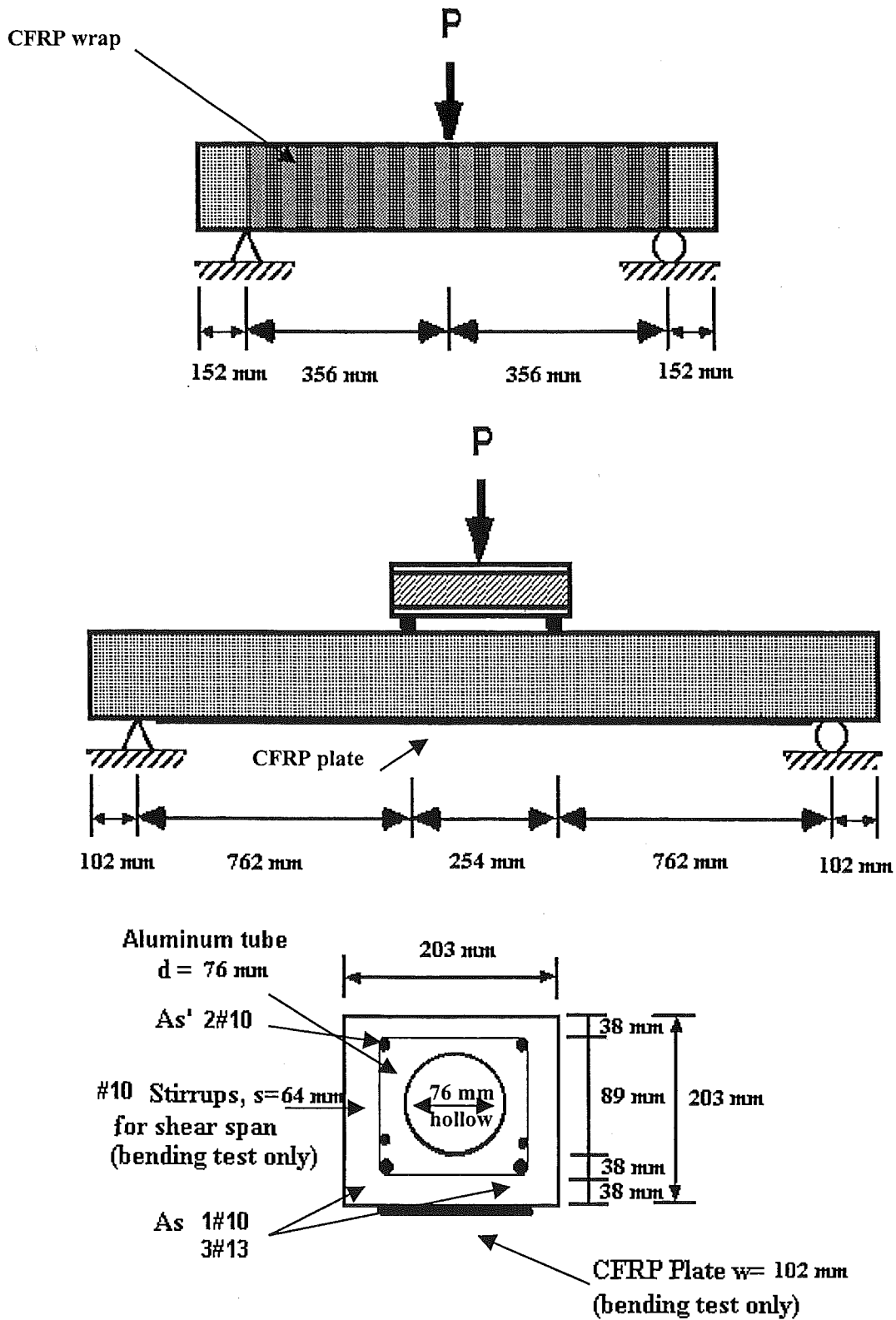
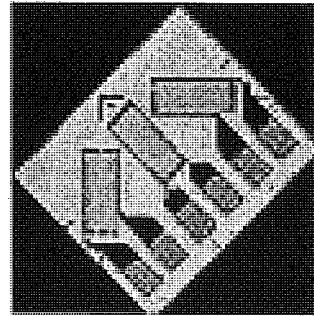
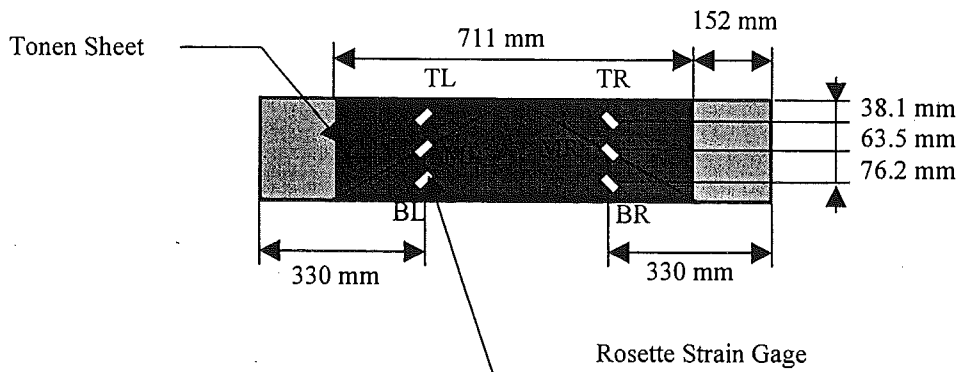
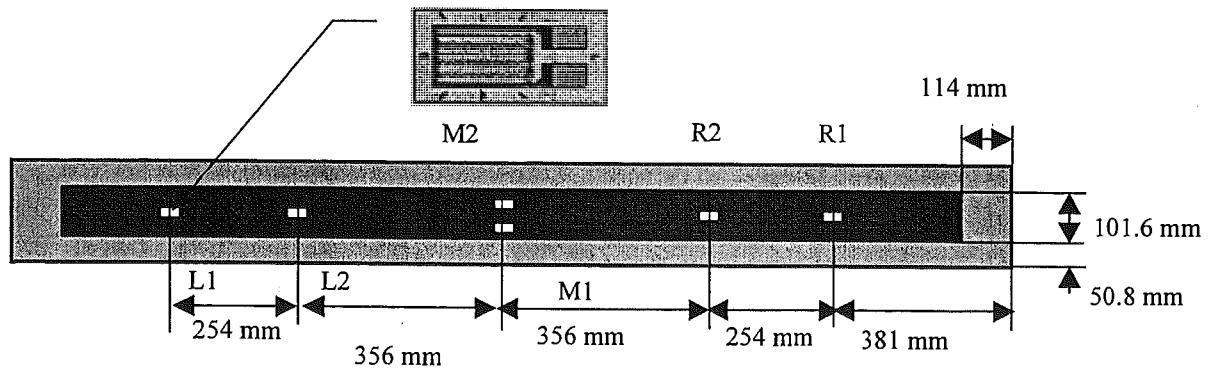


Figure 2.1 Cross Section and Load Set-Up for Shear (top) and Bending (bottom) Test



Shear Specimen Strain Gage Layout

1/4 Bridge Strain Gage



Bending Specimen Strain Gage Layout

Figure 2.2 Strain Gage Layout for the Shear and Bending Tests

3. DESIGN OF TEMPERATURE CONTROL SYSTEM

A temperature control system was designed to regulate the internal specimen temperature. The desired nominal temperature of specimens during testing specified by the project proposal was -29 degrees Celsius. Cooling was achieved by delivering liquid nitrogen into the core of hollow beam specimens, as shown in Figure 3.1. This concept was developed and implemented. The temperature control system instrumentation used to carry out the experiment is described in this section. A brief analysis and discussion of the performance of the cooling system is also included.

3.1. Liquid Nitrogen Cooling System

3.1.1. Specimen Cooling Apparatus

After preparing steel reinforcing cages, each specimen was fitted with a 76 mm diameter aluminum tube (see Figures 3.1 and 3.2). The tubes ran along the long axis of the beam and were held in place with steel wire. The tubes functioned as coolant reservoirs.

The coolant selected was Liquid Nitrogen (N_2). Although the boiling point of liquid nitrogen is much lower than the required temperature of -29 degrees Celsius, the extreme cold temperature allowed quick and efficient cooling of the specimens. The nitrogen was delivered through 12.7 mm diameter soft copper tubes. Several holes were drilled in the copper tubes to distribute the liquid nitrogen into the specimen. Both ends of the aluminum reservoir were capped with plywood plugs and 12.7 mm of concrete. Inlet and outlet plugs in these caps allowed for adding of liquid nitrogen and venting of excess nitrogen gasses. Two inlet tubes were used for the bending specimens, one at each end, and one inlet tube was used for the shear specimens because of the short span. The cooling system configurations for bending specimens and shear specimens are shown in Figures 3.3 and 3.4 respectively.

The flow of nitrogen into the specimen was controlled using a cryogenic rated solenoid valve. The solenoid valve had two states, open and closed. A duty cycle was established to control the flow rate of liquid nitrogen into the system.

3.1.2. Automatic Liquid Nitrogen Delivery System

The primary temperature control mechanism was the cryogenic rated solenoid valve mentioned in the above section. This valve was an integral part of the closed loop control system that regulated the specimen temperature. The system was comprised of three parts: a type "T" thermocouple, a computerized Proportional Integral Derivative (PID) controller, and a valve actuator, see Figure 3.5.

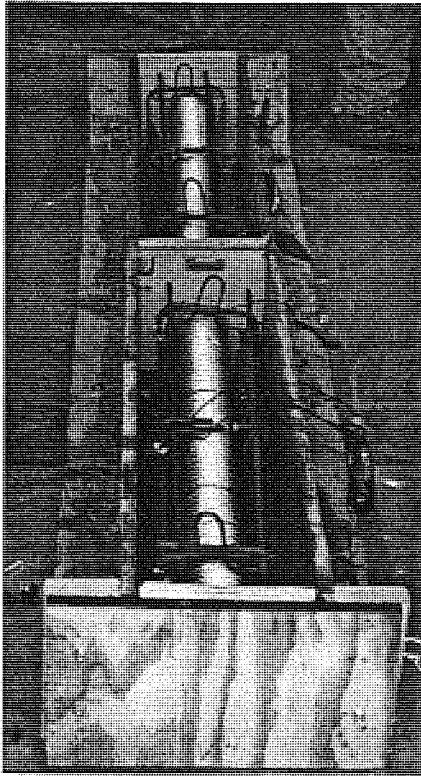


Figure 3.1 Photograph of the Hollow Shear Specimens before Concrete Pouring

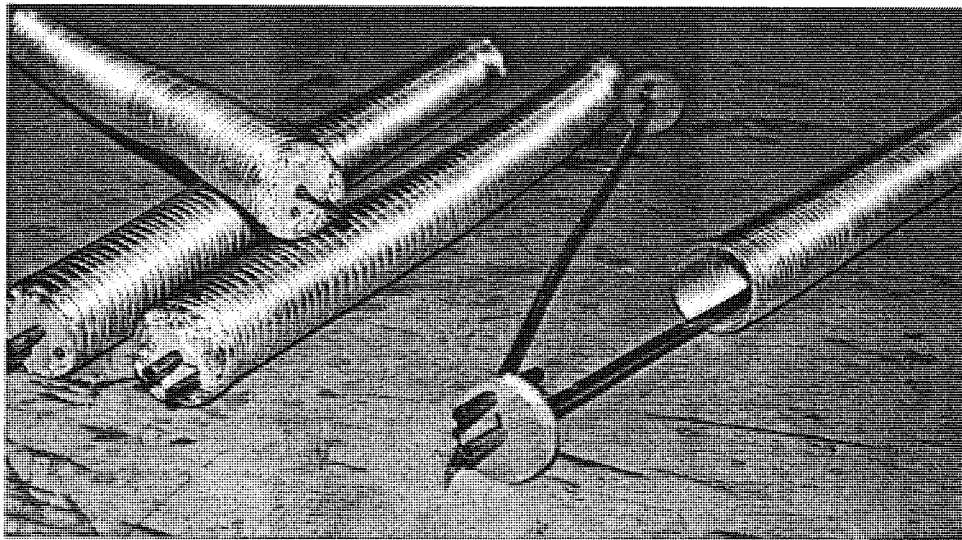


Figure 3.2 Photograph of Coolant Tubes

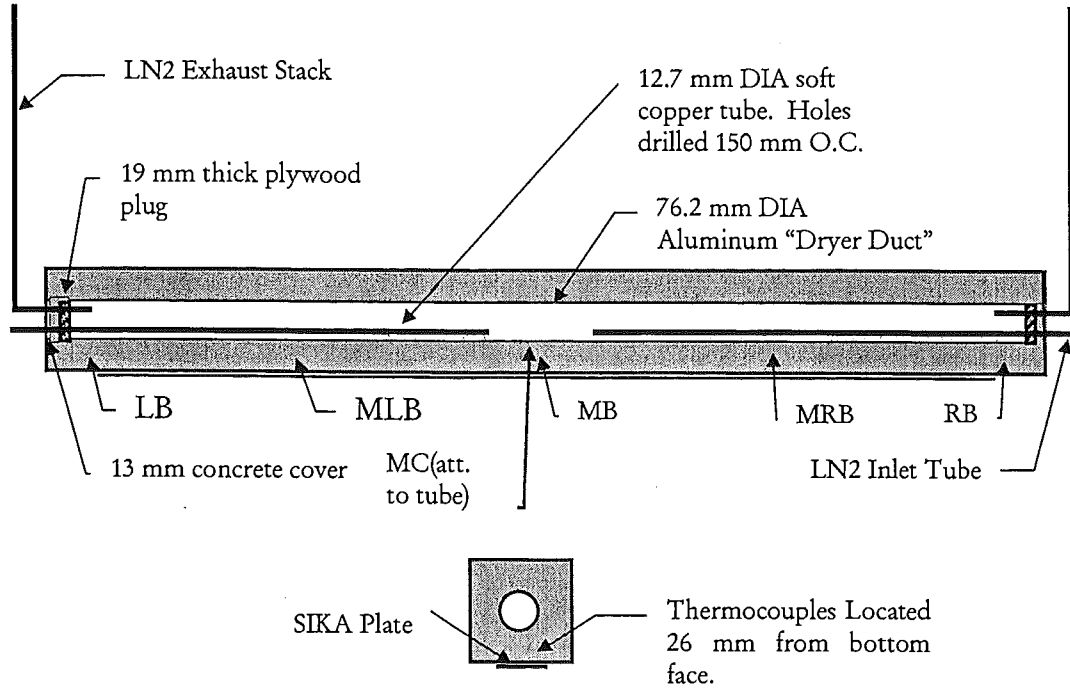


Figure 3.3 Flexural Specimen Cooling System.

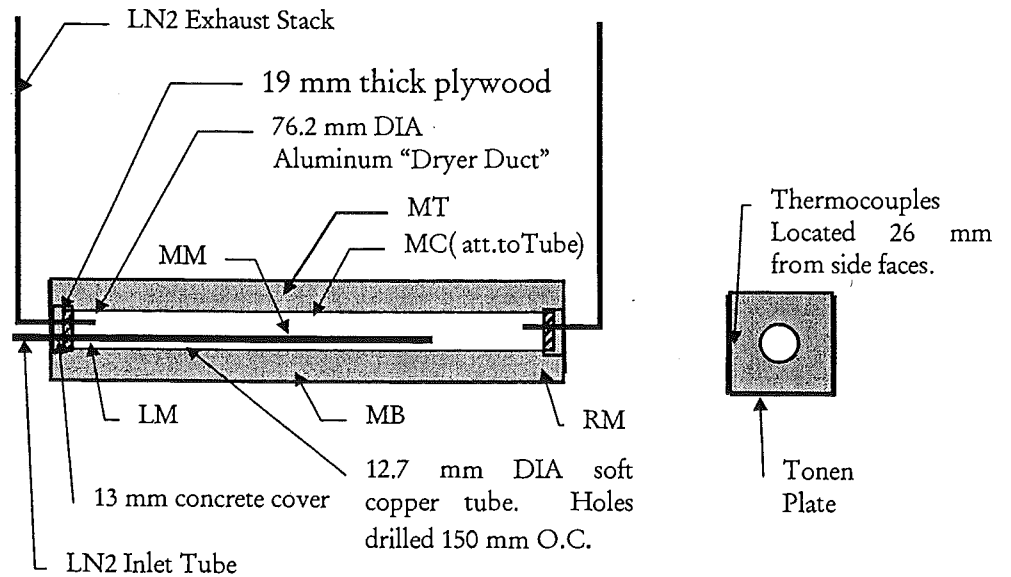


Figure 3.4 Shear Specimen Cooling System.

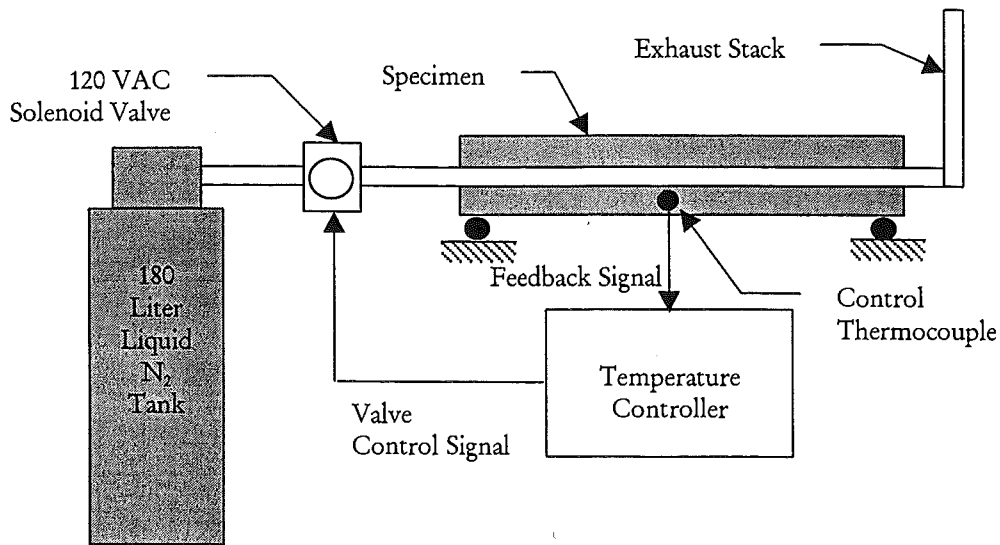


Figure 3.5 Temperature Control Loop

Several thermocouples were embedded in each specimen so differences in the temperature throughout the beam could be measured. The following notation was used to label the thermocouples: LB (left bottom), MLB (middle left bottom), MRB (middle right bottom), RB (right bottom), LM (left middle), RM (right middle) and MC (middle center). All thermocouples were located at a depth of 26 mm from the exterior surface of the beam with the exception of thermocouple MC (middle center). This thermocouple was mounted directly on the cooling tube. The locations of the thermocouples are shown in figures 3.3 and 3.4. One of these thermocouples fed temperature data to the computerized controller. The controller compared this data to user defined target temperature (set-point) and sent an appropriate command signal to the valve. The locations of the thermocouples are shown in Figures 3.3 and 3.4. The center bottom (MB) thermocouple was used for control of the bending specimen temperature because the area of interest was the interface between the CFRP and the concrete at the bottom of the beam. The center-side face (MM) thermocouple was used for the shear specimen because we were interested in the interface between the CFRP and the side surface of the beam.

3.1.3. *Insulation*

A foam insulation system was constructed to increase cooling efficiency and to decrease the thermal gradient between the core and outside surfaces of the specimens. The exterior surfaces of each specimen were fitted with a 25.4 mm thick layer foam insulation. The joints were sealed using spray foam insulation. Notches were cut in the insulation at 100 mm intervals to prevent the foam from having any effects on the strength of the beam. In addition to insulating the specimen, the external coolant tubes were wrapped with standard foam pipe insulation.

After the insulation system was installed, a significant improvement in cooling performance was measured.

3.1.4. Performance

The control of temperature in the area of interest (center bottom for flexure and center side for shear) was good. The coolant “pooled” at the extreme ends of the specimens causing lower temperatures in these regions. To decrease this effect, valves were placed on each exhaust stack to balance the flow of exhaust between the two sides of the specimens. Table 3.1 summarizes the average temperatures of the specimens at the controlled point during testing.

Table 3.1 Control Thermocouples and Average Temperatures

Specimen	Controlling Thermocouple.	Temperature Range	Average Temperature
Shear Monotonic	MM (Middle- Side Face)	-31.1 to -23.3 ° C	-27.1° C
Shear Cyclic	MM (Middle-Side Face)	-31.6 to -24.5 ° C	-28.9° C
Flexural Monotonic	MB (Middle-Bottom)	-30 to -28.9 ° C	-29.5° C
Flexural Cyclic	MB (Middle-Bottom)	-28.9 -27.8 to ° C	-28.3° C

Table 3.1. shows that the liquid nitrogen cooling system effectively cooled the beam specimens to the levels specified by the experimental program. Although the temperature was not one hundred percent uniform across the length of the beam, the temperature at the critical areas of the beam was controlled with a high degree of accuracy (+/- 5° C). For the experimental program, it was decided the performance of the system was acceptable.

4. TEST RESULTS

Table 4.1 presents a summary of the test results from the 4 beams tested, along with the predicted failure loads. Peak load, maximum shear force and maximum moment at failure and failure modes are reported for each beam. Figures 4.1 to 4.4 show the load versus deflection curves for each specimen. For the specimens tested under fatigue load, selected cycles are plotted. In order to visualize these graphs, the origin of the x axis was shifted by 2.5 mm for each of the fatigue curves.

Table 4.1 Summary of the Test Results

Beam	Parameter	Predicted load (KN)	Peak Load (KN) Range (%)	Max. Shear (KN)	Max. Moment (KN-m)	Type of Failure
1	Shear Monotonic	246	206	103	37	Concrete shear crack from load point to supports. Debonding of the CFRP sheet along the major crack.
2	Shear Fatigue	N.A.	20.6-165 10-80%	82.4	29	Total # cycles = 43083 Fatigue failure of the bottom layer of steel. A vertical crack of the entire concrete section and rupture of the CFRP sheet under the load point.
3	Flexure Monotonic	93	131	65.7	50	Partial debonding of the CFRP plate. Interfacial delamination of the CFRP plate at the extreme end.
4	Flexure Fatigue	N.A.	13.1-105 10-80% *9.4-75%	52.6	40	# of cycles = 85,000
		N.A.	13.1-118 10-90% *9.4-85%	59.1	45	# of cycles = 61,000 Total # cycles = 146,000
		N.A.	13.1-131 10-100% *9.4-94%	65.7	50	# of cycles = 9,500 Total # cycles = 155,500
		93	Monotonic 139.15	69.6	53	Total # cycles = 155,500 Partial debonding of the CFRP plate. Interfacial delamination of the CFRP plate at the extreme end. Crushing of concrete at the top layer midspan.

* Modified range according to maximum load of the monotonic test of the "fatigue" specimen.

N.A. Not Applicable.

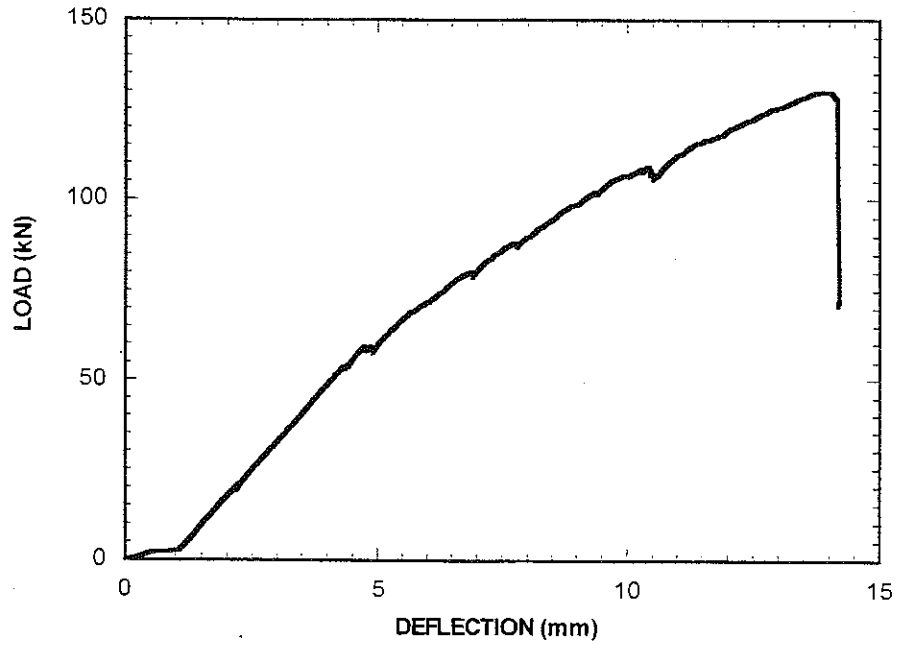


Figure 4.1 Load versus Deflection Curve for Monotonic Bending Test

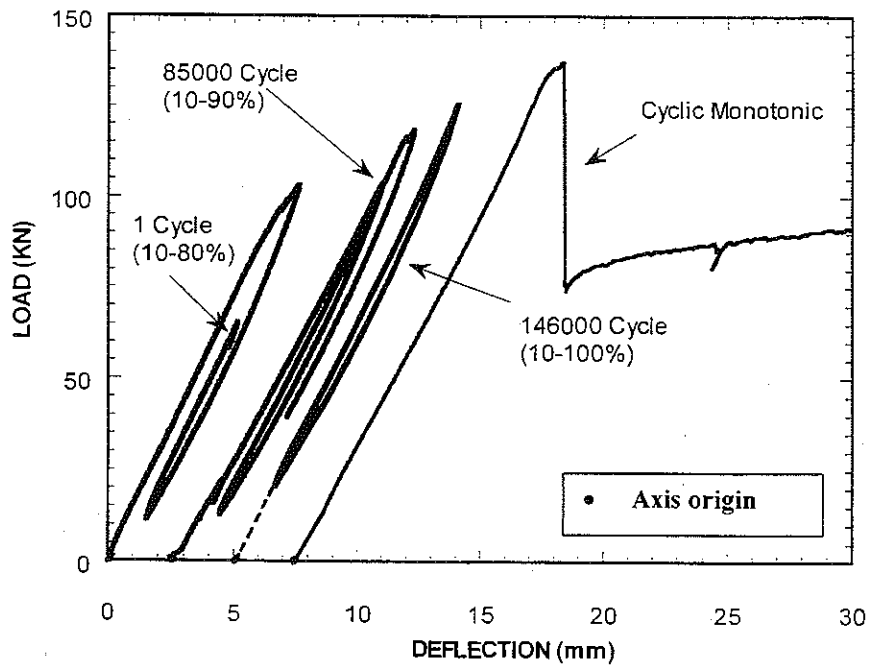


Figure 4.2 Load versus Deflection Curves for Fatigue Bending Test

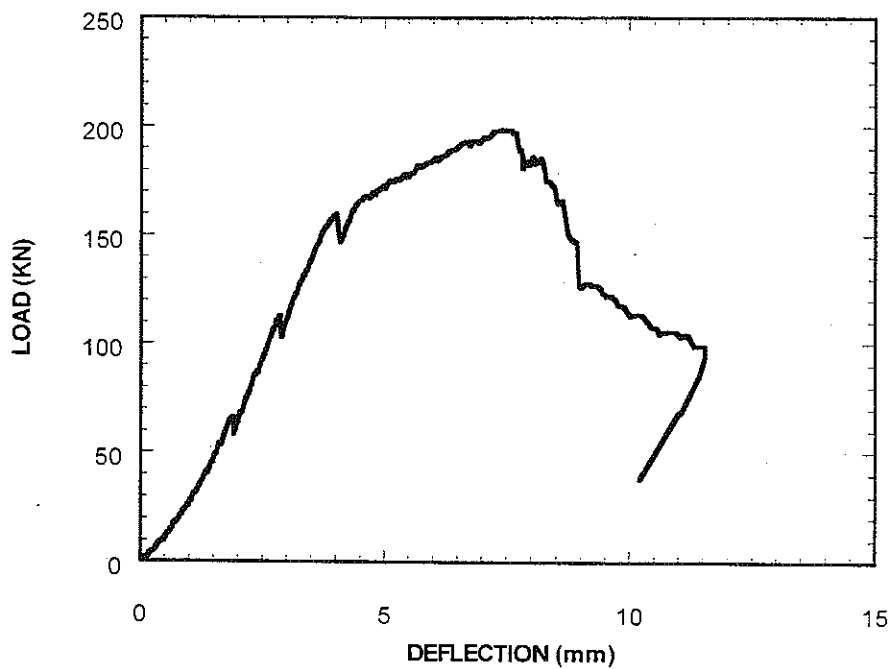


Figure 4.3 Load versus Deflection Curve for Monotonic Shear Test

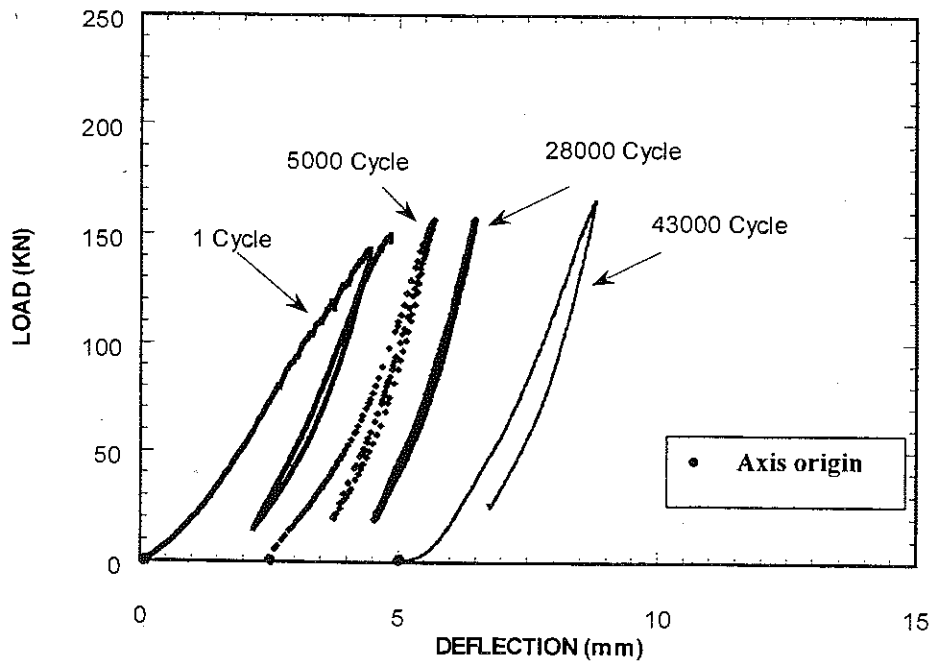


Figure 4.4 Load versus Deflection Curves for Fatigue Shear Test

5. ANALYSIS AND INTERPRETATION

5.1. Steel Reinforcement Ratio

Since the concrete compressive strength of the specimens at the day of testing varied from the target value of 34.5 MPa, the steel reinforcement ratio also varied from the value of $2/3$ of ρ_{max} . Table 5.1 shows the new value of the steel reinforcement ratio.

Table 5.1 Summary of the Test Results

Beam Parameter	Day of Testing	f'_c (MPa)	Steel Reinf. Ratio
Shear Monotonic	15 days	23.24	$0.89 \rho_{max}$
Shear Fatigue	15 days	23.24	$0.89 \rho_{max}$
Flexure Monotonic	21 days	24.13	$0.85 \rho_{max}$
Flexure Fatigue	60 days	30.49	$0.70 \rho_{max}$

As can be seen from Table 5.1, the steel reinforcement ratio for all specimens is higher than the value of $2/3 \rho_{max}$. However, since it doesn't exceed the value of ρ_{max} , the specimens satisfy AASTHO requirements.

For the flexure specimens, the difference in concrete compressive strength between the date of monotonic testing and fatigue testing was 26%, while the difference between the maximum failure load between the monotonic and the fatigue-monotonic test was 6%. It can be concluded that this variation of the compressive strength does not affect significantly the strength of the strengthened beam.

5.2. Failure Modes

5.2.1. Flexure Test

As was observed in the bending tests of Task 2, beams reinforced with Sika plates failed in all cases by partial debonding of the CFRP plate. For the current flexure tests, failure was also by partial debonding of the CFRP Sika plate. This type of failure has been associated with interfacial shear failure between the surface of the concrete and the CFRP plate. The epoxy adhesive between them tore out the concrete just above the interface epoxy/concrete. The debonding length for both cases was around 1060 mm (60% of the bonded CFRP length), extended from the zone of maximum moment to one of the ends of the CFRP plate. There was no evidence of variation of the failure mode due to the effect of the fatigue cycles. It was also found that at the debonded end of the CFRP plate, interlaminar failure (failure within the

laminate) was also present. It is presumed that the release of energy due to debonding may have contributed to this type of failure at the end of the CFRP plate. A closer observation of this phenomenon revealed that only a first layer of single fibers was kept bonded to the adhesive. Therefore this type of failure can still be considered as interface failure (Concrete-epoxy interface).

Figure 5.1 and 5.2 show photographs of both the debonding and the interfacial failure for the monotonic flexure test. In this test, debonding seems to have started at the left shear span of the beam next to the left point load. Figure 5.3 shows the load-strain curves. Strain gage L1 was reported damaged and did not record any data. Strains at strain gage L2 significantly decreased at about 110 KN reflecting the occurrence of a debonding process on the proximity of its location. A redistribution of the stresses happens at this level showing an increase in the strain rate for the remaining strain gages.

The flexural beam subjected to cyclic fatigue loading also failed by partial debonding of the Sika CFRP plate. After 155,500 cycles, the beam was tested under monotonic load up to failure. As shown in Figure 5.4 and 5.5 the same type of failure observed for the monotonically tested beam was also observed for this beam. Debonding process also seems to have started on the right shear span. The length of the interlaminar failure within the laminate was 3 times larger (300 mm) than the one obtained from the monotonic test. Note that the total debonding length was about 1060 mm for both cases. The damage of the CFRP plate is more evident, several layers of fibers were separated from the original plate, see Figure 5.6. Figure 5.7 shows the load-strain curves for the monotonic loading test after cycling. Strain gage R1 shows increments of strains up to the failure load, after that point, the strain level registered was the lower of all, indicating that debonding has occurred on this side of the beam. For strain gage R1 the strain rate was higher than for L1. This presence of higher end plate stresses is also related with the presence of the interlaminar failure at this location. Strain gage R2 failed after the maximum load. All the other strain gages also registered a drop of strain at failure.

5.2.2. Shear Test

The monotonic shear beam failed by propagation of a major diagonal crack (shear failure) from the load point to one of the supports (left side). Debonding of the CFRP sheet occurred along this crack due to the relative displacement of the two concrete blocks. Figure 5.8 and 5.9 show photographs of this type of failure. The strain gage rosettes placed on the surface of the Tonen CFRP sheet registered a very small amount of strain. It was also found that the type of epoxy used to glue the rosettes to the surface of the CFRP lost its full bonding properties with the low temperature. Therefore some of the rosettes used did not register strain. Figure 5.10 shows same load versus shear strain curves for this test. It can be seen that the strain gages on the left side registered significant jumps. These "jumps" are associated to propagation of the shear crack along the concrete beam and the corresponding debonding of the CFRP sheet.

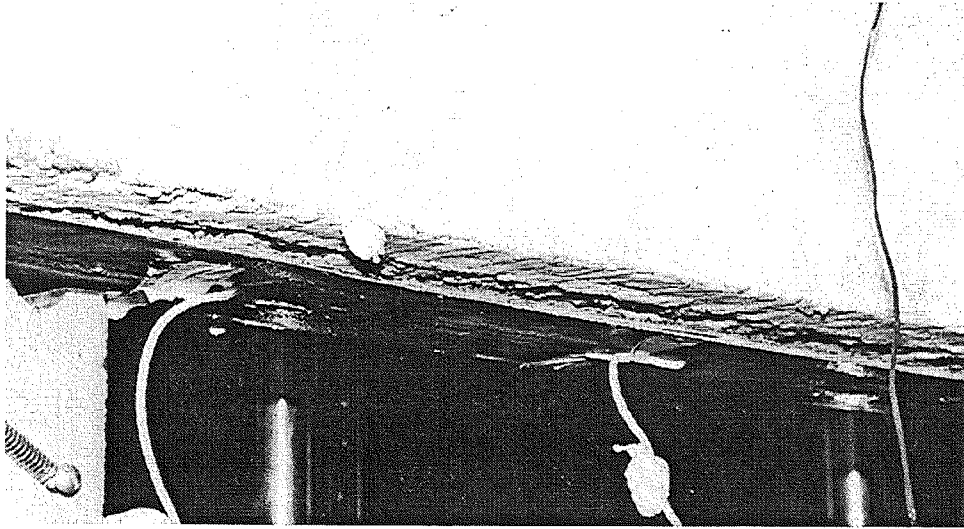


Figure 5.1 Interfacial Failure of the Monotonic Bending Specimen

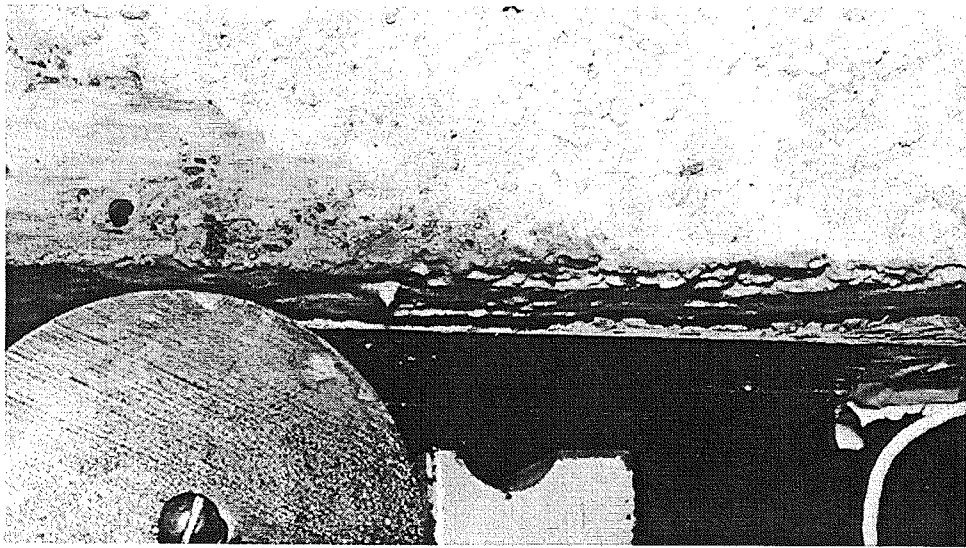


Figure 5.2 Detail of the Interfacial Failure of the Monotonic Bending Specimen

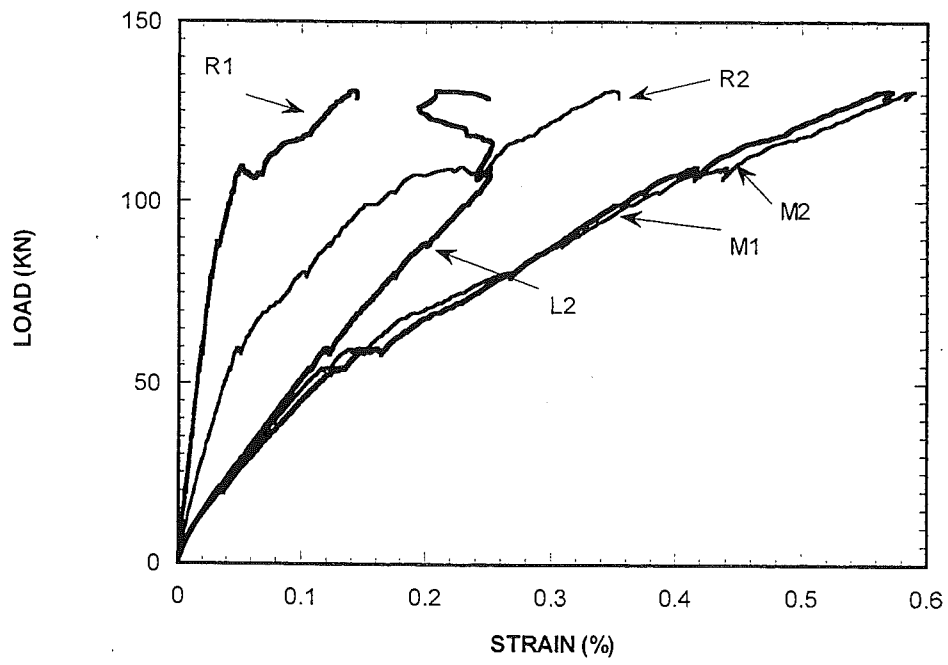


Figure 5.3 Load versus Strain Curves for Monotonic Flexure Test

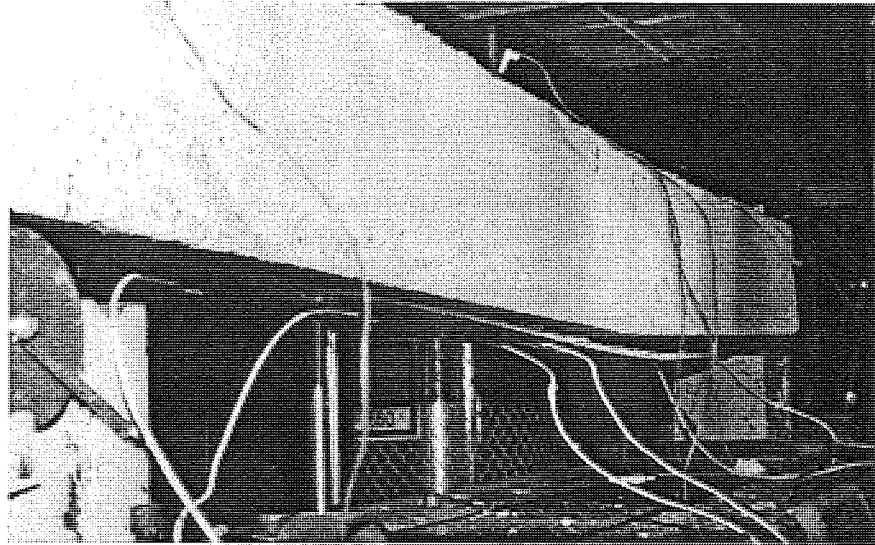


Figure 5.4 Interfacial Failure of the Fatigue Flexure Test

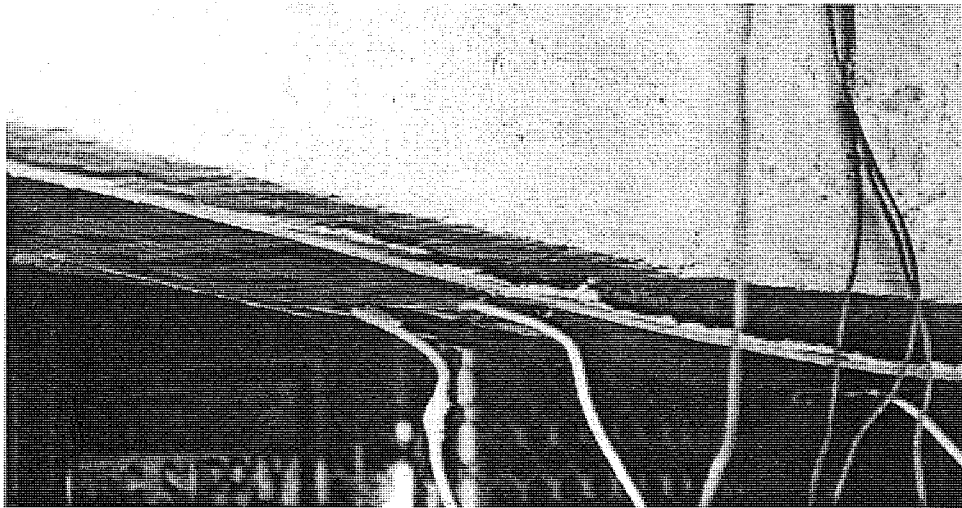


Figure 5.5. Detail of the Interfacial Failure (Fatigue Flexure)



Figure 5.6 Interlaminar Failure at End of the Sika Plate (Fatigue Flexure)

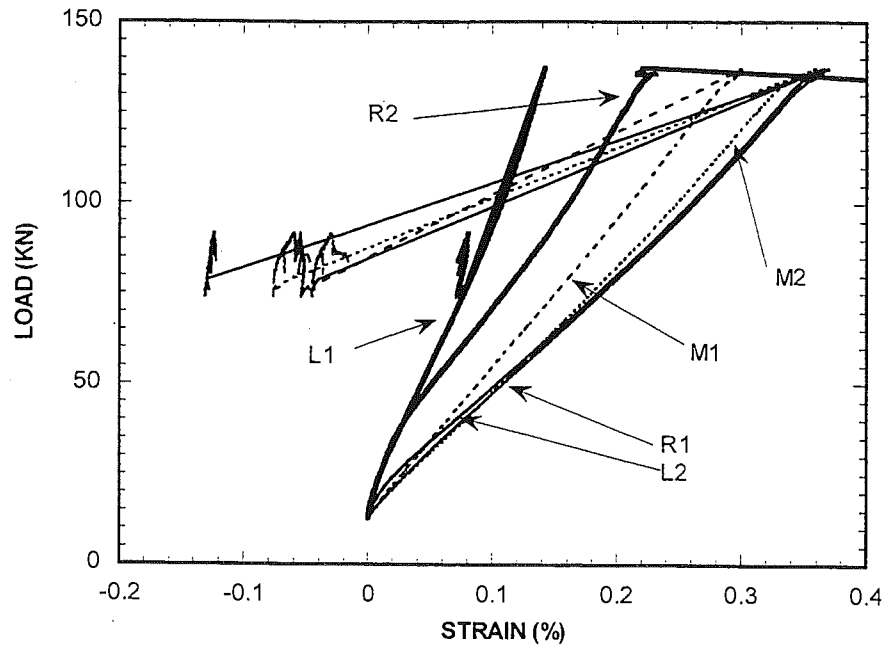


Figure 5.7 Load versus Strain Curves for Monotonic after Cycling Flexure Test

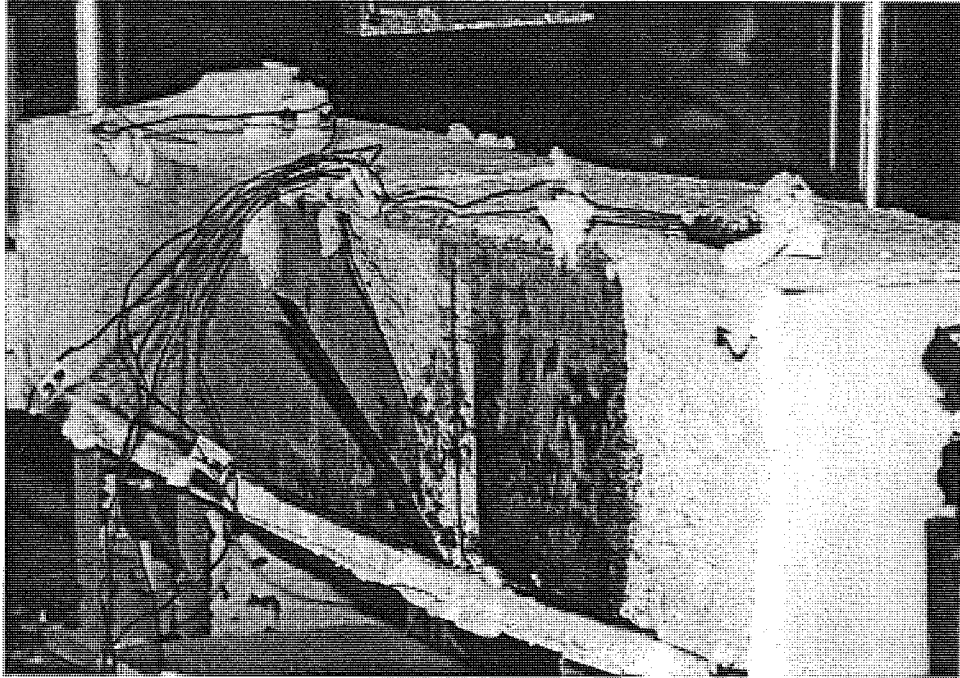


Figure 5.8 Shear Failure and Debonding of the Tonen CFRP sheet (Shear Monotonic)

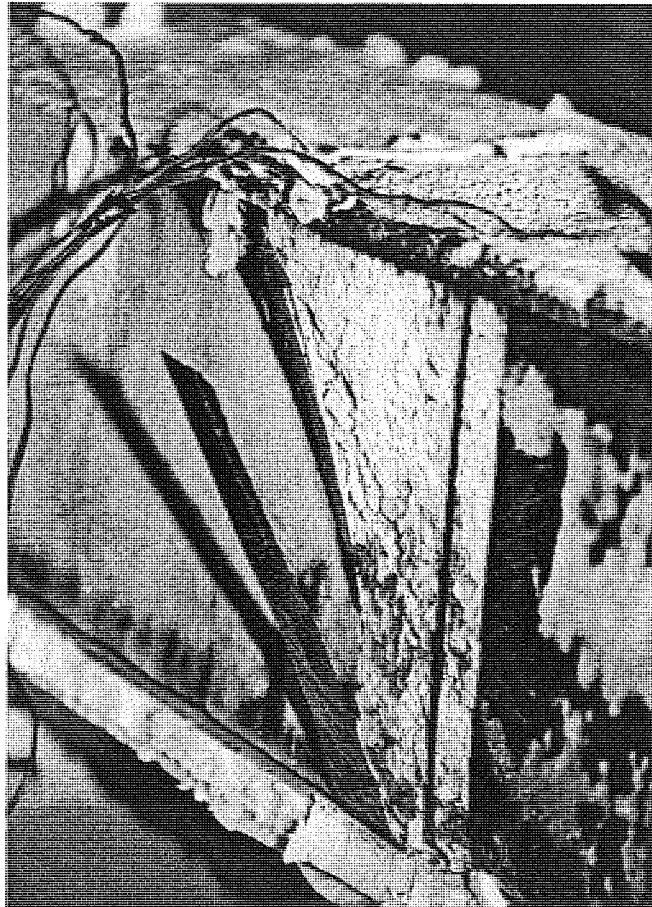


Figure 5.9 Detail of the Debonded Area (Shear Monotonic)

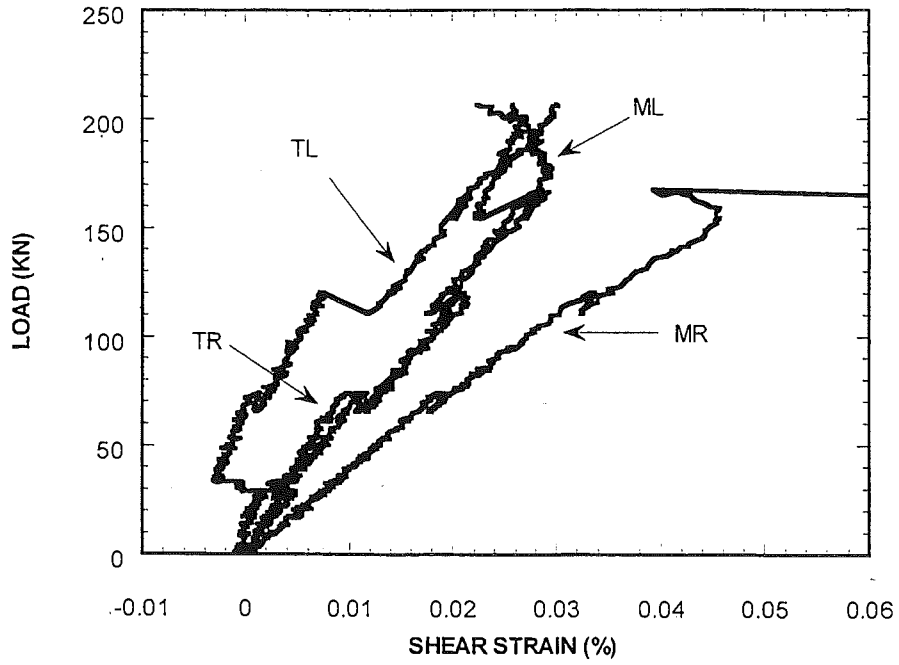


Figure 5.10 Load versus Shear Strain Curves from the Monotonic Shear Test

From Figure 5.10 it can be seen that neglecting these “jumps” the shear strains on the CFRP would have a linear relationship with the load. The shear strains are higher at the midsection than at the top of the CFRP wrap as is expected from the shear distribution of strains along the cross section of a RC beam.

The specimen subjected to fatigue cycles under shear load configuration failed by fatigue of three of the reinforcing bars in the extreme layer of reinforcement under the load point. A major vertical crack developed in the concrete at the midspan section including the CFRP sheet. Figures 5.11 and 5.12 show photograph of this test. Samples of the rebars that failed were analyzed under the microscope. Figure 5.13 and 5.14 show photographs of the surface of two coupons. A radial orientation of the grains of steel indicates a brittle failure. It was assumed that a small fatigue crack could initiate a brittle fracture of the section with low temperatures. Even if the type of failure of this specimen was different from the monotonic shear test, it is not considered representative of the overall behavior of a reinforced concrete beam using CFRP sheets as shear reinforcement. A beam with no stirrups is expected to behave in a brittle manner, especially when subjected to fatigue loads. In this particular configuration the longitudinal rebars were the only element able to perform load redistribution. If they fail, no load redistribution is possible and the beam will fail. Figure 5.15 shows the load-shear strain curves from the shear fatigue test. Similar to the monotonic test, shear strains are higher at the middle than at the top of the CFRP wrap. Except for the strain at the middle left, shear strains showed a linear relationship with the load.

5.3. Strengthening Level

Load versus deflection curves for the flexure tests were presented in Figure 4.1-4.2. A comparison is presented in Figure 5.16. As indicated previously for a better visualization of these graphs, the different fatigue curves were scattered along the deflection axis (i.e. origin was shifted on the x axis). From Figure 5.16 it is shown that under fatigue loads, the stiffness of the beam after 155500 fatigue cycles is higher than for the monotonic case. From the preliminary calculations, it was expected that the moment capacity of this section was 35.54 N-m and the CFRP will take a maximum stress of 745 MPa at failure (see last row of table 1A, Appendix a). From the experimental data, it was found that the maximum moment capacity of the beam was 50 N-m, a difference of 30% with the preliminary analysis.

As was predicted on the preliminary calculations, debonding of the laminate occurred before the full strength of the laminate could be reached. Figure 5.17 shows load-stress curves for the monotonic case, based on the strain values obtained from the strain gages (see Figure 5.3) and the CFRP modulus provided by the manufacturer. From this figure it can be observed that maximum stresses at mid span were 885 MPa, only 37% of the maximum strength capacity of the Sika laminate (2400 MPa). This experimental value (885 MPa) was 20% higher than the one predicted in Appendix A (734 MPa).

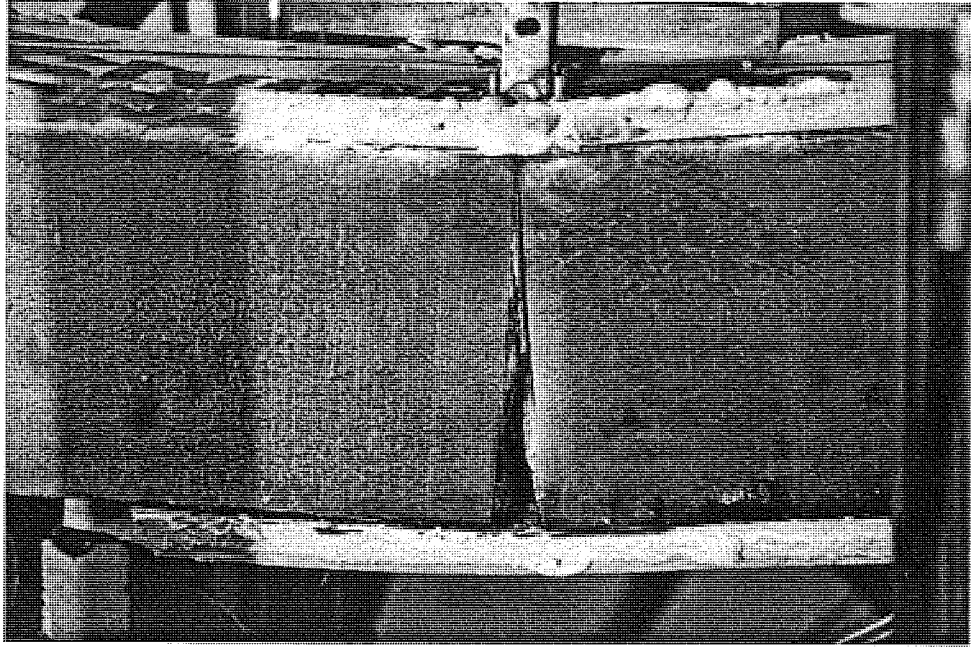


Figure 5.11 Fatigue Failure of the Shear Cyclic Specimen

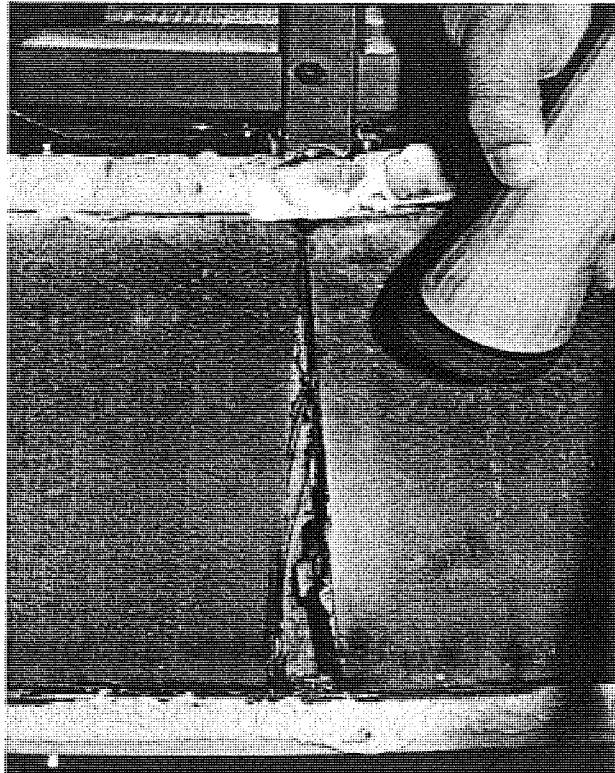


Figure 5.12 Detail of the Fatigue Failure of the Shear Cyclic Specimen

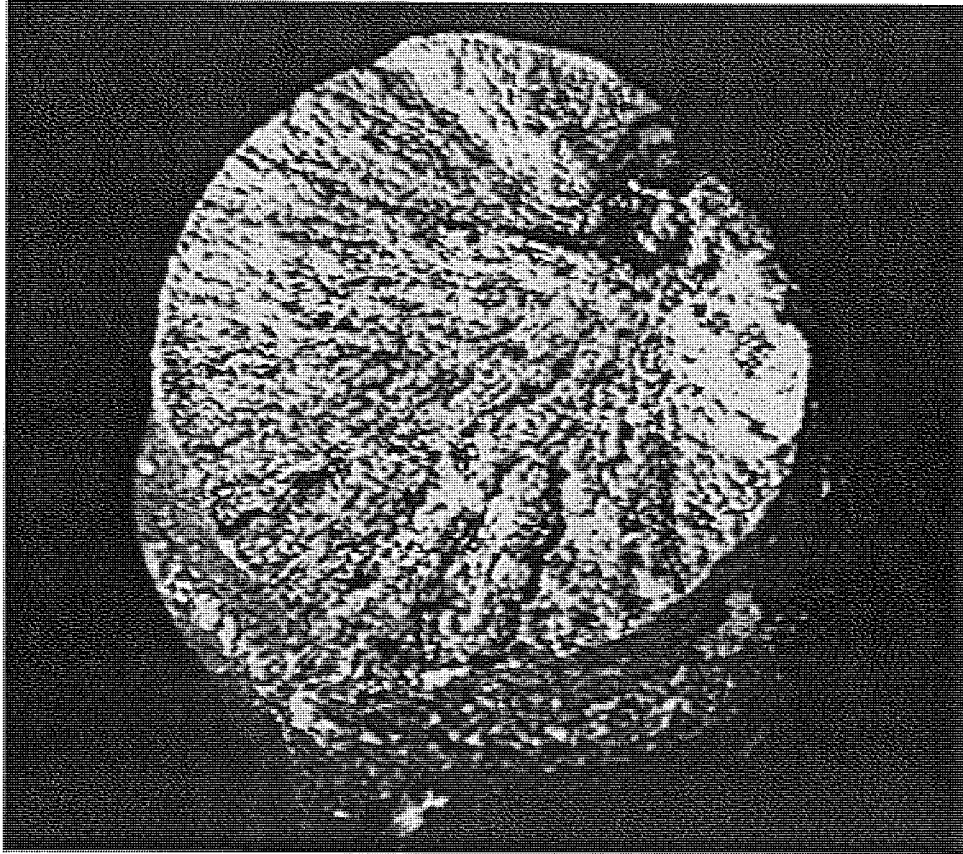


Figure 5.13 Fatigue Failure of a Steel Rebar (bar No.10)

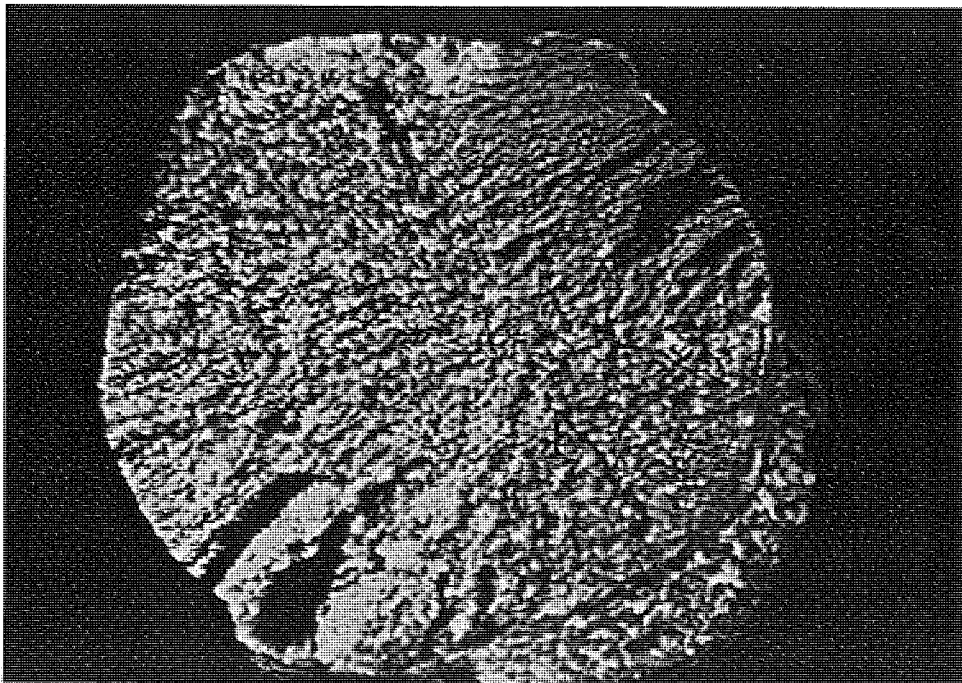


Figure 5.14 Fatigue Failure of a Steel Rebar (bar No. 13)

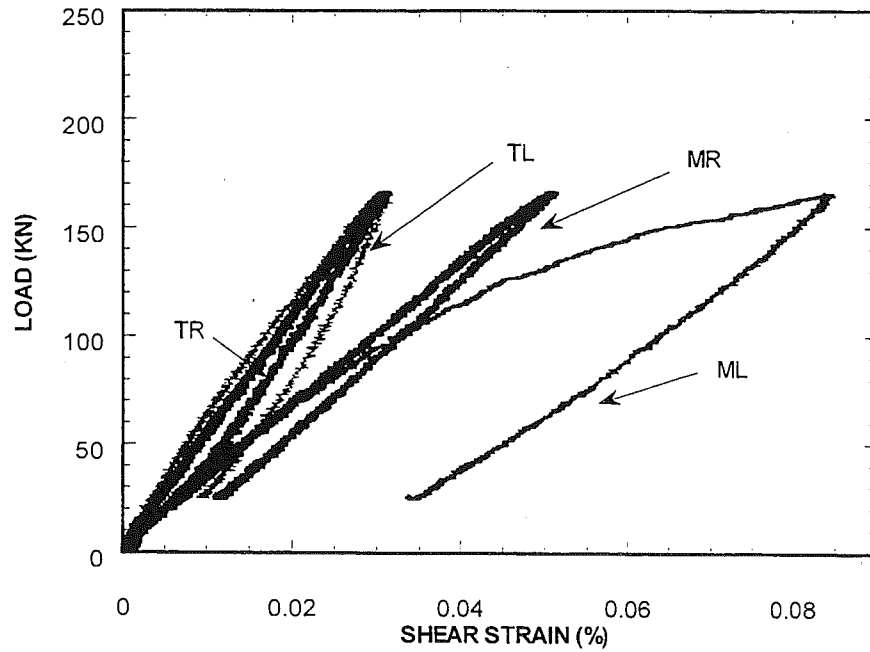


Figure 5.15 Load versus Shear Strain Curves from the Fatigue Shear Test

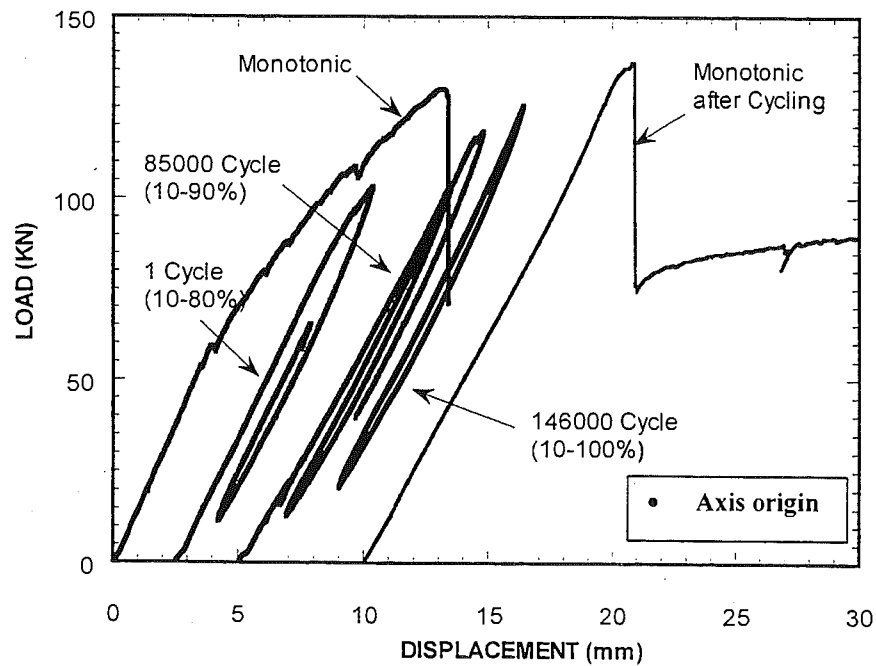


Figure 5.16 Load versus Deflection Curves for Monotonic and Fatigue Bending Tests

Using this experimental value of maximum strain, interfacial shear stress(τ_s) can be calculated as:

$$\tau_s = (\sigma_{CFRP} * t_f) / l_d, \sigma_{CFRP} = E_{CFRP} e_{CFRP}$$

where l_d is the length of the shear span and σ_{cfRP} is the average stress of the CFRP sheet at the midspan and t_f is the thickness of the CFRP plate.

For the monotonic case, the value of τ_s is equal to 1.39 MPa, a higher value than the one predicted in Appendix A ($\tau_s=1.15$ MPa).

For the cyclic monotonic case, strain gages registered a maximum value of 554 MPa at the right end (R1), see Figure 5.18. The stress value at this point was only 23% of the maximum strength capacity. Strain gages placed at the midspan (M2) and the left side (L2) registered maximum strain values very close to the one registered by strain gage R1. This graph is an indication that a redistribution of stresses has occurred within the laminate probably due to the presence of some debonding along the interface, giving a more uniform pattern than the one registered on the monotonic case.

Since the maximum value of stress at the CFRP level was found at one of the ends, three different calculations for the value of the interfacial shear stress were carried out. The first calculation takes the average maximum stress value registered at the midspan times the area of the laminate and divides it by the total length of the shear span. This is a conservative calculation approximation since it is based on the assumption that the entire shear span will carry a uniform shear stress (as was calculated for the case of the monotonic bending specimen). The second calculation takes into account that the shear stress may not be uniform along the span and that partial debonding failure occurred at the end of the laminate and not at midspan. For the monotonic test, maximum stress value registered by L2 is multiplied by the area of the laminate and divided by the surface area from that point up to the end ($l=521$ mm). For the cyclic test, maximum stress value registered at R2 is multiplied by the area of the laminate and divided by the surface area from that point up to the end ($l=521$ mm). Finally, a strip of beam of the length equal to the distance between two strain gages located on the shear span ($l=254$ mm) is considered. The difference between the stresses in the laminate (L1-L2 and R1-R2) is used to calculate the value of τ ($l=254$ mm). Table 5.2 presents a summary of these calculations.

Table 5.2 Interfacial Shear Values for the Bending Tests

	τ , MPa (experimental, midspan)	τ , MPa experimental , ¼ span)	τ , MPa (experimental left span-right span)
Monotonic flexure	1.39	0.87	N.A. *1.62
Cyclic flexure	0.79	0.76	*1.58 1.05

*debonding failure occurred at this span

N.A. = value not available due to failure of strain gage L1.

It can be determined from the calculations presented above, all the τ values calculated from a difference between the values given by the strain gages located on the shear span that failed gave the higher value of the interfacial shear stress. Interfacial shear values calculated from the average stresses of the CFRP at the midspan represent a lower limit of this value. This table shows that the interfacial shear stress is not uniform along the shear span and that presence of high end plate stresses may influence the location of the debonding area.

For the shear tests, both monotonic and fatigue, the maximum capacity of the specimen was defined by the shear confinement that the CFRP sheets could confer to the beam. According to AASHTO, the shear contribution given by the concrete can be estimated as $V_c = 0.17\sqrt{f_c} bd$. For a $f_c = 23.24$ MPa, this contribution is equal to 23 KN. Even though the strain readings revealed a low stage of strains on the surface of the CFRP wraps, indirect findings can be analyzed. Figure 5.10 shows the load-shear strain curves from the shear monotonic test. It can be seen that the first jump in all the curves is present at a load of 28 KN and correspond to the initiation of the first shear crack on the concrete. This value fits well with the theoretical concrete shear strength calculated above.

From the shear tests, shear stresses were calculated from the values of shear strain provided by the strain gages rosettes (see Figures 5.10 and 5.15) and a value of 4.40 GPa for the shear modulus found in the literature review [XX-48], see Table 5.3.

Al-Sulaimani et al. [XX-43] present an equation to evaluate the shear contribution of the CFRP wrap. It is assumed that peeling of the wrap will occurred when the maximum shear stress τ_{max} reaches the interface shear strength τ_{ult} ($\tau_{ult} = 3.5$ MPa). The shear distribution is assumed to be parabolic with maximum at the top and bottom of the strip. Value of τ_{ave} (average) can be estimated from the experimental results:

$$V_p = 2(\tau_{ave} (d*hw)/2)$$

where V_p is the shear contribution of the CFRP wrap ($V = V_p + V_c$), d = distance from extreme compression fiber to centroid of steel reinforcement and hw = depth of the strip.

Assuming $V_c = 23$ kN, values for V_p and τ_{ave} were calculated. Experimental shear stresses as well as values for τ_{ave} are presented in Table 5.3.

Table 5.3 Shear Contribution of the CFRP sheet

Source	Parameter	Monotonic Shear Test	Fatigue Shear Test
Experimental	CFRP Shear contribution, N	$V_p = 80$ KN	$V_p = 60$ KN (at the moment of failure)
[XX-43]	Interfacial shear stress, τ_{ave} , MPa	2.77	2.08
Calculated*	$\tau = G \times$ shear strain, MPa	1.89(max)0.92(min)	3.70(max)1.32(min)

* Shear strains were obtained from experimental results, shear modulus G was found in the literature review.

From the monotonic test, it can be seen that the Toner CFRP sheet wrapped around three sides of the beam gave an additional shear capacity of 80 KN. A maximum shear strain (0.045%) was obtained for the strain gage rosette located on the middle right side. The shear stress at this level is equal to 1.89 MPa. Following the equation given by [XX-43] the bond strength of the interface

between the CFRP laminate and the concrete was found to be 2.77 MPa which is 3.4 times the shear strength of the concrete ($0.17\sqrt{f_c}$). Confidence of the data collected by the strain gages rosettes is being doubted due to the presence of bond failure of the strain gages.

For the cyclic test, the bond between the strain gage and the CFRP surface also seems to be deteriorated even more notoriously by the combined effect of the cold temperature and fatigue. Figure 5.15 shows selected load-strain curves for the last fatigue cycle. Two strain gages failed early on the test. However, from the data collected, it was found that a maximum shear strain (0.084%) was obtained for the strain gage rosette located on the middle left side. The shear stress at this level is equal to 3.70 MPa. Following the equation given by [XX-43] the bond strength of the interface between the CFRP laminate and the concrete was found to be 2.08 MPa which is 2.5 times the shear strength of the concrete ($0.17\sqrt{f_c}$).

5.4. Temperature and Fatigue Effect

In this part of the study, no control beam was tested under room temperature; thus it is not possible to make a quantitative assessment of the effect of cold temperature on the overall behavior of the specimens. However, a qualitative evaluation can be made in comparison to previous bending and shear tests carried out at room temperature.

From the previous bending tests, all the beams tested had a longitudinal reinforcement ratio smaller than the beam tested at low temperature. For a beam with a longitudinal reinforcement of $0.54 \rho_{max}$ and 1 strip of Sika Carbodur of 100 mm (beam No.8-1), the failure load was 33% higher than the control beam. The Sika plate had a maximum tensile stress of approximately 600 MPa (25% of the maximum strength capacity of the laminate). The bending beam tested monotonically under low temperatures had a failure load 120% higher than the theoretical moment capacity of the beam without the CFRP reinforcement. The Sika plate had a maximum tensile stress at midspan of 885 MPa (37% of the maximum strength capacity of the laminate). It can be concluded that the low temperatures did not affect the flexure strengthening level provided by the Sika system.

For the bending tests at low temperatures, the same failure mode was observed also for beams tested at room temperature. Debonding of the laminate due to shear failure of the interface between the CFRP and the concrete led to a premature failure of the beam since it did not allow the CFRP to reach its maximum strength.

It can be concluded that no evident effect of the cold temperature is observed for the Sika strengthening system.

From the previous shear tests, a beam with a longitudinal reinforcement of $1.41 \rho_{max}$, no stirrups and wrapped with 1 layer of the Tonen sheet (beam No. 2) obtained a failure load 150% higher than the control beam. The shear beam tested monotonically at low temperature ($0.89 \rho_{max}$, no stirrups and wrapped with 1 layer of the Tonen sheet) had a failure load 800% higher than the predicted shear concrete strength. It can then be conclude that the low temperatures did not affect the shear strengthening level provided by the Tonen system.

For the shear beam tested monotonically at low temperature, failure was similar to that observed in the previous shear tests at room temperature. Propagation of a major concrete shear crack from the load point to one of the supports (left side) led to debonding of the CFRP sheet along this crack due to the relative displacement of the two concrete blocks. The shear specimen subjected to cyclic fatigue loads failed by brittle failure of three of the reinforcing bars in the extreme layer of reinforcement. It was considered that a combination of low temperature and fatigue could have contributed to this type of failure. However, since this failure was by the steel rebars, one can also conclude that there was no evidence that cold temperature had an effect on the Tonen strengthening system.

Other effects of fatigue loading can be observed by comparison with specimens tested under monotonic load.

Comparing load-strain curves for the monotonic and last cycle of the fatigue bending test, it can be observed that a redistribution of stresses and strain has occurred along the CFRP plate. A higher number of flexural cracks were observed under fatigue. Due to the fact that the beam was insulated all the time, it was not possible to observe deterioration of the interfacial layer. Calculated values of the interfacial shear stress were always lower for the case of fatigue test than for the monotonic test with a minimum and maximum difference of 3-40%. It was concluded that fatigue cycles at low temperatures decrease the strength of the interface between the CFRP laminate and the concrete.

For the shear tests, because fatigue at low temperature led to failure of rebars, there was no evidence of fatigue on the CFRP sheet. Shear strains registered on the surface of the CFRP at the top height were at the same level as those for the monotonic case indicating no deterioration of bonding at this level. At the mid height of the CFRP sheet, an increase in shear strain was recorded with an increasing number of fatigue cycles. It was expected that deterioration of the bond between the CFRP wrap and the concrete surface at this level, probably related to the fatigue failure of the steel rebars allowed a larger deformation of the CFRP sheet under fatigue load.

Finally it was concluded that the interface between the CFRP laminate and the concrete is the weakest link of this strengthening system and is likely to first register effects of low temperature and fatigue load.

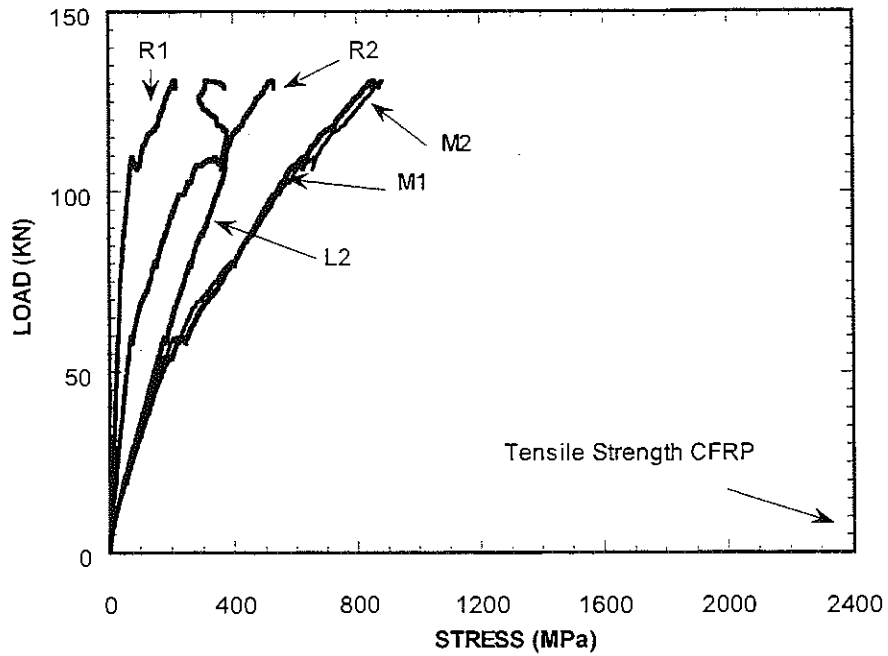


Figure 5.17 Load versus Stress Curves for Monotonic Flexure Test

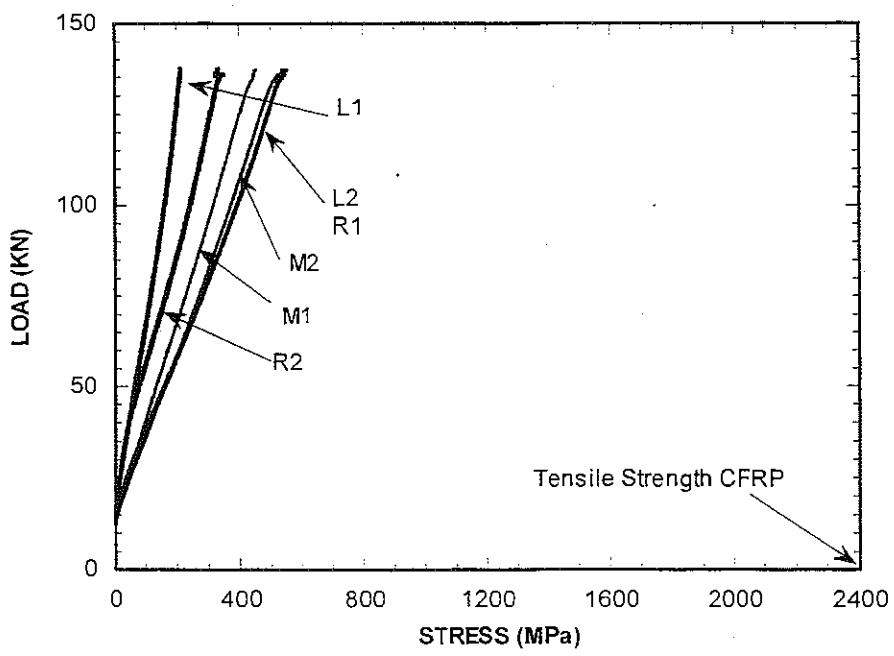


Figure 5.18 Load versus Stress Curves for Monotonic after Cycling Bending Test

6. CONCLUSIONS

1. Prior tests (Task 2) showed that the failure mode of RC beams strengthened with CFRP Sika plates and loaded in monotonic bending at normal room temperature was by delamination of the CFRP plate. The limited tests carried out in this task with low temperature (-29 °C) and cyclic fatigue loading, suggest that the failure mode remains the same, that is by delamination.
2. The strain data of the cyclic fatigue test in bending showed redistribution of strains (thus stresses) in the CFRP plate with an increasing number of cycles. A more uniform strain pattern was achieved suggesting that slow delamination of the plate occurred during cycling. Higher strains at the end of the plate confirmed the extension of delamination toward that section and subsequent delamination failure at that section.
3. Values of the interfacial shear stress from the strains recorded by the gages showed that the interfacial strength at failure (1.62-1.58 MPa) was similar for both the monotonically flexure tested beam and the fatigue flexure beam after 155500 cycles
4. Failure in the shear beam subjected to monotonic loading at -29 °C occurred by shear delamination of the CFRP Tonen sheet followed by shear failure of the concrete. The shear delamination was due to the propagation of a diagonal shear crack within the concrete that extended from the load point to the support.
5. Failure in the shear beam that was subjected to cyclic fatigue loading at -29 °C was initiated by failure of one of the reinforcing bars in the first layer of steel, and shortly followed by failure of two additional bars. Subsequent analysis suggested that failure of the rebars was by brittle fracture due to the low temperatures at which the tests were preformed.
6. Increase in the shear strain obtained with cyclic shear loading from the rosette gage placed at midspan along the vertical axis of the beam suggest that some delamination and cracking were occurring at that section. It is likely that a shear failure would have occurred in a manner similar to the monotonically tested beam, should failure of the reinforcing bar not have occurred.

7. REFERENCES WITH SOURCE CLASSIFICATION

SOA - State of the Art Reports & Review Documents

- SOA-1. "State-of-the-art Report on Fiber Reinforced Plastic (FRP) Reinforcement for Concrete Structures". ACI Committee 440, 1996.
- SOA-2. "US Research Projects", International Research on Advanced Composites for construction (IRACC-96), Bologna, June 9-11, 1996.

SCD - Sika (Carbodur)

- SCD-7 "Engineering Guidelines for the use of Sika Carbodur (CFRP) laminates for structural strengthening of concrete structures." Commercial material from Sika Corporation. First Edition, August 1997.

CAN - Canadian Institutes and Universities

- CAN-1. Soudki Khaled and Green Mark F. "Performance of CFRP Retrofitted Concrete Columns at low Temperatures". From Proceeding of the Advanced Composite Materials in Bridges and Structures. Canadian Society for Civil Engineering, Montreal, Quebec, 1996.
- CAN-2. Hoa S.V., Xie M. and Xiao X.R. "Repair of Steel Reinforced Concrete with Carbon/Epoxy Composites" From Proceeding of the Advanced Composite Materials in Bridges and Structures. Canadian Society for Civil Engineering, Montreal, Quebec, 1996.
- CAN-3. Baumert M.E., Green M.F. and Erki M.A. "A Review of low Temperature Response of Reinforced Concrete Beams strengthened with FRP sheets". From Proceeding of the Advanced Composite Materials in Bridges and Structures. Canadian Society for Civil Engineering, Montreal, Quebec, 1996.

EMPA - Swiss Federal Laboratories for Materials Testing and Research

- EMPA-1. Meier U., "Strengthening of Structures Using Carbon Fibre/Epoxy Composites", Construction and Building materials, Vol.9, No.6, pp.341-351, 1995.

DE - University of Delaware, Delaware Department of Transportation

- DE-1. Chajes M.J., Thomson T.A., Januszka T.F., Finch W.W., "Flexural Strengthening Of Concrete Beams Using Externally Bonded Composite Materials".1994.
- DE-2. Chajes, M.J., Mertz, D.R., Thomson, T.A., and Farschman, C.A., "Durability of Composite Material Reinforcement," Proceedings of the Third Materials Engineering Conference on Infrastructure: New Materials and Methods of Repair, Kim, D.B., Editor, ASCE, 1994, pp. 598-605.
- DE-5. Chajes, M. et al, "Shear Strengthening of Reinforced concrete Beams using Externally Applied Composites Fabrics," ACI structural Journal. V.92, No. 3. May-June 1995. Pp. 295-303.

XX - Other Research Institutions

- XX-9 Gomez J., Casto B., "Freeze-Thaw Durability of Composite Materials", 1st International Conference Composites in Infrastructure, ICCI, Tucson, Arizona, January 1996, pp.947-955.
- XX-26 Rahman R.H., Taylor, D.A., and Kingsley C.Y., "Evaluation of FRP as Reinforcement for Concrete Bridges," Proceedings of International Symposium on FRP Reinforcement for Concrete Structures, Nanni, A., and Dolan, C., Editors, ACI, SP-138, Detroit, 1993, pp. 71-80.
- XX-27 Shulley, S.B., Huang, X., Karbhari, V.M., and Gillespie, J.W., "Fundamental Consideration of Design and Durability on Composite Rehabilitation Schemes for Steel Girders with Web Distress," Proceedings of the Third Materials Engineering Conference on Infrastructure: New Materials and Methods of Repair, Kim, D.B., Editor, ASCE, 1994, pp. 1187-1194.
- XX-46 Blaschko M., Niedermeier R., and Zilch K., "Bond Failure Modes of Flexural Members Strengthened with FRP", Proceeding of the Second International Conference on Composites in Infrastructure, H. Saadatmanesh and M.R. Ehsani, Editors, Tucson, AZ 1998, pp. 315-327.
- XX-43 Al-Sulaimani G, et al., "Shear Repair for Reinforced concrete by Fiberglass Plate Bonding," ACI Structural Journal, V.91, no. 3, july-August 1994. Pp. 458-464.
- XX-47 Arduini M., Di Tommaso A., Nanni A., "Brittle Failure in FRP Plate and Sheet Bonded Beams", ACI Structural Journal, V. 94, No. 4, July-August 1997, pp.363-370.
- XX-48 Hyer Michael W., "Stress Analysis of fiber Reinforced Composite Materials", Mc. Graw-Hill publishers. ISBN 0-07-016700-1. 1998. Page 58.

APPENDIX A

Design of Reinforced Concrete Beams with CFRP for Low Temperature Test

Design of the reinforced concrete beams strengthened with the CFRP sheets was defined prior to the experimental tests. Expected maximum load was necessary to select the load cell to be used for the experimental load set-up. It was also desired to obtain the highest strengthening level that the CFRP plate could provide for a given steel reinforcement level.

Calculation of reinforcement ratio for reinforced concrete beam with no CFRP

$$\rho_b = \frac{0.85\beta_1 f'_c}{f_y} \times \left(\frac{\epsilon_{cu}}{\epsilon_{cu} + \epsilon_y} \right) = 0.00249, f'_c = 24.13 \text{ MPa}$$

$$\rho_{\max} = 0.75\rho_b$$

$$A_s = 3\#13 + 1\#10 = 458 \text{ mm}^2,$$

$$\rho = 0.0159 = 0.85\rho_{\max}$$

$$\text{Moment Capacity} = 22.64 \text{ kN-m}$$

Moment Capacity for RC beam with CFRP plate

A spreadsheet provided by Sika Corporation was used to design the RC beam strengthened with a layer of CFRP plate. According to Sika Co., this spreadsheet is based on experience of European manufacturers and has been calibrated with ACI fundamentals. The design methodology follows the strain compatibility method where the concrete stress-strain curve is built according to the Swiss code (SIA 162, 1989)[SCD-7]

For a particular RC beam (geometry, steel reinforcement ratio, steel yield strength, concrete compressive strength already defined), the spreadsheet can provide moment value, concrete strain, steel strain and CFRP strain for a particular percentage of the ultimate moment capacity. Delamination of the CFRP plate is also checked according to a procedure developed by the Swiss Federal Laboratories for Material Testing and Research (EMPA). A copy of the print-out of the spreadsheet is provided at the end of this section.

For the defined bending beam, different widths of Sika plate were input into the spreadsheet. Moment capacity was defined as the moment when the top compressive concrete strain is equal to 0.003. It was also checked that steel had yielded at this level. Strain at the level of the CFRP plate was calculated as well as the expected development length required by this methodology.

Following the uniform shear model developed in the freeze-thaw report (report from task No.4) appendix A, shear stresses at the concrete-CFRP interface were calculated. Also,

assuming a interfacial shear strength of $\tau_1=0.17\sqrt{f'_c} = .813$ MPa and $\tau_2=0.34\sqrt{f'_c} = 1.63$ Mpa (assumed as feasible range of values for the shear strength of the interface based on previous bending tests) , development length is checked for every case.

Since the shear forces are uniform in the shear span of a four point bending test, a uniform interfacial shear stress (τ_s) model is considered.

$$\text{Therefore } l_d = T_{\text{CFRP}} / (b * \tau_s) = (\sigma_{\text{CFRP}} * t_f) / \tau_s \quad \sigma_{\text{CFRP}} = E_{\text{CFRP}} e_{\text{CFRP}}$$

$$\tau_s = (\sigma_{\text{CFRP}} * t_f) / l_d$$

where l_d is the development length and $T_{\text{CFRP}}, \sigma_{\text{CFRP}}$ are the tensile force and stress of the CFRP sheet at the point under one of the concentrated loads, b and t_f are the width and thickness of the CFRP plate and τ_s is the shear strength of the interface. To calculate τ_s , l_d was assumed as the shear span for the CFRP laminate and σ_{CFRP} is calculated from the strain of the CFRP for every case. To calculate l_d , τ_s is set equal to τ_1 and τ_2 , and σ_{CFRP} is calculated from the strain of the CFRP for every case.

Summary of the results of this design is presented in Table 1A. A Sika plate of a width equal to 102 mm is chosen for a shear span length of 762 mm. A wider CFRP plate will lead to compressive failure on the top concrete layer. A narrower CFRP plate will fail by delamination giving a lower moment capacity. This final selection is checked following the strain compatibility design methodology presented in the freeze-thaw report. It is found that this selection provide an interfacial shear stress of 1.15 MPa, which is between the range giving by τ_1 and τ_2 , data. Results of this calculation are also presented in Table 1A.

Table 1A. Summary of Design Calculations

Sika plate Width (mm)	Moment (kN-m)	Yield of steel reinf.	Strain of CFRP plate	Interf. Shear stress (MPa)	Shear span (mm)	Development length (mm) for the Sika plate		
						Software	(τ_1)	(τ_2)
25.4	31.18	Yes	0.00759	1.84	762	1727	1727	864
51.0	35.25	Yes	0.0065	1.58	762	1270	1473	737
76.0	39.32	Yes	0.00542	1.31	762	889	1219	610
102	40.67	Yes	0.00433	1.05	762	559	991	508
127	43.38	Yes	0.0043	1.05	762	559	991	508
152	42.03	No	0.00325	0.79	762	508	991	508
178	44.74	No	0.00325	0.79	762	508	762	381
203	48.80	No	0.00325	0.79	762	508	762	381
*102	35.54	Yes	0.00474	1.15	762	N.A.	N.A.	N.A.

*revised final design values

N.A. not applicable

Design of stirrups

Stirrups (#10 close stirrup) were provided for the shear force at the ultimate moment capacity calculated previously. AASTHO provisions were considered for the amount and spacing of the stirrups. Figure 1A shows the stirrup layout for this specimen.

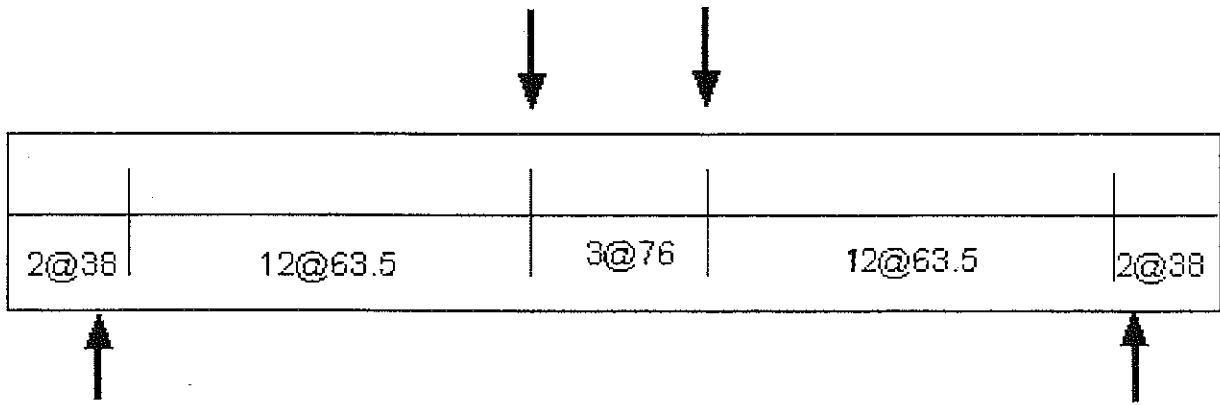


Figure 1A. Stirrup Layout for the Bending Test

Shear Capacity for RC beams wrapped with CFRP sheets

Different researchers have evaluated in a different way the contribution of the CFRP wraps to shear reinforcement. Since the peeling-off effect is present on both tests fatigue and cyclic, it is therefore necessary to evaluate this effect in the calculation of the shear confinement. [XX-43] presents an equation to evaluate the shear contribution of the CFRP wrap. It is assumed that peeling of the wrap will occurred when the maximum shear stress τ_{max} reaches the interface shear strength τ_{ult} ($\tau_{ult} = 3.5$ MPa). The shear distribution is assumed to be parabolic with maximum at the top and bottom of the strip. V_p is the shear contribution of the CFRP wrap defined by:

$$V_p = 2(\tau_{ave} (d \cdot h_w) / 2)$$

where τ_{ave} is the average value of the shear strength over the height of the wrap.

Assuming $V_c = 0.17\sqrt{f'_c} bd$, $V_c = 23$ kN (for $f'_c = 24.13$ MPa)

Assuming $\tau_{ave} = \tau_{ult} = 3.5$ MPa $V_p = 100$ kN

The total shear capacity of the section (V) is calculated as: $V = V_c + V_p = 123$ kN

